A direct link between the global regulator PhoP and the Csr regulon in *Y. pseudotuberculosis* through the small regulatory RNA CsrC

Aaron M. Nuss[+], Franziska Schuster[+], Ann Kathrin Heroven, Wiebke Heine, Fabio Pisano, and Petra Dersch*

Department of Molecular Infection Biology,
Helmholtz Centre for Infection Research, 38124 Braunschweig, Germany

*Corresponding author:
Petra Dersch
Dept. of Molecular Infection Biology,
Helmholtz Centre for Infection Research
38124 Braunschweig, Germany
Phone: +49-531-6181-5700
FAX: +49-531-6181-5709
e-mail: petra.dersch@helmholtz-hzi.de

[+]These authors contributed equally to this study.

Running title: PhoP activates *csrC* expression in *Y. pseudotuberculosis*
Keywords: *Y. pseudotuberculosis,* virulence gene regulation, PhoP, regulatory RNAs, Csr system, RovA

Abstract

In this study we investigated the influence of the global response regulator PhoP on the complex regulatory cascade controlling expression of early stage virulence genes of *Yersinia pseudotuberculosis* via the virulence regulator RovA. Our analysis revealed the following novel features: (i) PhoP activates expression of the CsrC RNA in *Y. pseudotuberculosis,* leading to activation of RovA synthesis through the CsrABC-RovM cascade, (ii) activation of *csrC* transcription is direct and PhoP is shown to bind to two separate PhoP box-like sites, (iii) PhoP-mediated activation results in transcription from two different promoters closely downstream of the PhoP binding sites, leading to two distinct CsrC RNAs, and (iv) the stability of the CsrC RNAs differs significantly between the *Y. pseudotuberculosis* strains YPIII and IP32953 due to a 20 nucleotides insertion in $CsrC_{IP32953}$ which renders the transcript more susceptible to degradation. In summary, our study showed that PhoP-mediated influence on the regulatory cascade controlling the Csr system and RovA in *Y. pseudotuberculosis* varies within the species, suggesting that the Csr system is a focal point to readjust and adapt the genus to different hosts and reservoirs.

Introduction

Pathogenic bacteria, which circulate frequently between external habitats/reservoirs and warm-blooded hosts, are continuously confronted with rapidly changing environmental conditions, including variations of nutrients and ion concentrations, temperature, oxygen and pH. Within their hosts, the bacteria have to cope with competing microbiota and often very harmful situations, such as the attack of the host immune system aiming to eradicate invading pathogens. In order to ensure their survival and propagation, bacteria need to survey the changes of their local environment, transduce and translate the signals to respond adequately.

In bacteria, two-component regulatory systems serve as an external stimulus-response coupling machinery to convert specific environmental signals into a cellular response, typically by differential expression of multiple target genes. Generally, a histidine protein kinase and a response regulator form the basis of these modular and adaptable phosphotransfer-signaling schemes [1-3]. The pleiotropic PhoP/PhoQ two-component system constitutes one of the most crucial signal transduction systems controlling bacterial virulence [4-6]. The membrane-bound sensor kinase PhoQ responds predominantly to low environmental Mg^{2+} (but also to Ca^{2+} and Mn^{2+}), acidic pH, and host-secreted antimicrobial peptides, and phosphorylates the cytoplasmic response regulator PhoP [4]. Phosphorylated PhoP either activates or represses its target genes through binding to a conserved binding motif in the proximity of the target promoters [7-9], which is similar to the PhoP-box sequence of *E. coli* and *Salmonella* [10-12]. Most of the work on PhoP/PhoQ and its role for virulence has been carried out with *Salmonella* and *Yersinia* species. In both species PhoP/PhoQ promotes survival and proliferation in macrophages and neutrophils, as well as survival in the presence of antimicrobial peptides [4, 13-18]. A *phoP* knock-out mutant of *S. enterica* serovar Typhimurium was shown to be highly attenuated for virulence in

mice [4, 14, 19, 20]. The role of the PhoP/PhoQ system for virulence in *Yersinia* is less clear as conflicting results have been reported for different strains and infection models, but the overall defect of the *phoP* mutants in virulence is more modest compared to *Salmonella* [15, 21-24]. The phenotypic differences of the *phoP* mutants might reflect variations in the regulatory circuits and composition of the individual regulons. In fact, the PhoP/PhoQ regulons of *Y. pestis* and *S. enterica* are both complex and include many target genes, albeit the architecture of the PhoP-dependent promoters as well as the function of PhoP itself vary considerably between the two pathogens [25, 26].

The PhoP regulon members have been identified in *Y. pestis* biovar Microtus, which is supposed to be avirulent to humans. Several genes which are involved in detoxification, protection against DNA damage, resistance to antimicrobial peptides, and adaptation to magnesium limitation (e.g. *mgtCB* that encodes a Mg^{2+} transport system) were proven to be direct targets of PhoP [9, 27, 28]. Recent studies further showed that PhoP of *Y. pestis* biovar Microtus also acts as direct activator of *crp* and as repressor of the *rovA*, *psaEF* and *psaABC* loci [28, 29] which are all part of a complex regulatory cascade characterized in the close relative *Y. pseudotuberculosis* (Fig. **1**) [30].

RovA belongs to the SlyA/Hor/Rap family of MarR-type dimeric winged-helix DNA-binding proteins, controlling a wide range of physiological processes involved in environmental and host-associated stress adaptation and virulence in bacterial pathogens [31]. The RovA regulon includes multiple virulence-linked factors and their function is crucial for the pathogenicity of all three human pathogenic *Yersinia* species [32-36]. In the enteropathogenic *Yersinia* species, *Y. pseudotuberculosis* and *Y. enterocolitica*, RovA activates expression of *invA* which contributes to an efficient co-lonization of the Peyer´s patches and allows faster progression of the infection [34, 35,

[37]. A *Y. pestis* CO92 Δ*rovA* mutant is strongly attenuated (≈ 80-fold by LD_{50}) and colonization of spleen and lung in mice is abolished upon subcutaneous injection, whereas only a slight attenuation was observed when the pathogen was given via an intranasal or intraperitoneal route. This indicated that RovA plays a more important role in bubonic plague than pneumonic plague or systemic infection [33].

The *rovA* locus of *Y. pestis* and *Y. pseudotuberculosis* is 100% identical. It is transcribed by two promoters and is positively autoregulated in both pathogens [28, 38]. Expression of *rovA* is also strongly thermoregulated. This is based on the fact that RovA is an intrinsic temperature-sensing regulator in which thermally induced conformational changes interfere with DNA-binding capacity, and render RovA susceptible to proteolytic degradation [39]. In addition, *rovA* transcription was shown to be strongly influenced by the nutrient composition of the growth medium, and this is mediated by the Crp-CsrABC-RovM regulatory cascade (Fig. **1**) [30, 35, 40].

The global regulator Crp regulates uptake and catabolism of carbohydrates and was found to control expression of the two regulatory RNAs CsrB and CsrC in *Y. pseudotuberculosis* which are part of the carbon storage regulator (Csr) system [40, 41]. Both Csr RNAs harbor several GGA motifs, which promote binding/sequestration and inactivation of the global post-transcriptional regulator protein CsrA. Binding of CsrA typically blocks translation initiation of its target mRNAs and this is often accompanied by an accelerated mRNA decay [42, 43]. The CsrA recognition site seems to be quite variable; however a highly conserved GGA motif that is often present in the loop of short hairpins was found to be highly conserved (Dubey *et al*., 2005; Babitzke and Romeo, 2007).

Among the CsrA target mRNAs of *Yersinia* and other related pathogens are many classical virulence genes and regulators, but also multiple virulence-linked metabolic, physiological (e.g. motility) and stress adaptation traits [40, 41, 44].

In the present work, we studied the influence of PhoP on the complex CsrABC-RovM-RovA regulatory cascade in *Y. pseudotuberculosis* mediating the expression of important early stage virulence genes such as invasin. We found that PhoP activates *csrC* expression directly from two different promoters. The stability of the resulting CsrC RNAs differs significantly between the *Y. pseudotuberculosis* strains YPIII and IP32953, due to a 20 nucleotides insertion in the IP32953 CsrC RNA which renders the transcript more susceptible to degradation. Our work shows that the regulatory cascade controlling RovA can vary significantly between different *Y. pseudotuberculosis* isolates, suggesting evolutionary changes that adapt expression of the individual sets of pathogenicity factors to specific niches within hosts.

Results

PhoP activates *rovA* expression in *Y. pseudotuberculosis* via RovM

Previous work with *Y. pestis* demonstrated that the PhoP/PhoQ two-component system influences orthologues of two virulence regulators, Crp and RovA, controlling expression of important early stage virulence genes in the close relative *Y. pseudo-tuberculosis* (Fig. **1**) [28, 29]. In order to test the role of PhoP in *Y. pseudotuberculosis,* we first investigated the influence of the response regulator on RovA expression in the wild-type strains YPIII and IP32953. Both strains have most frequently been used to elucidate *Y. pseudotuberculosis* pathogenicity. However, recently it was found that YPIII carries a mutation in the PhoP-encoding gene YPK_1715, leading to a non-functional version of PhoP [45]. Therefore, we first constructed a set of isogenic *phoP*$^+$ and *phoP*$^-$ derivatives of YPIII and IP32953. To do so, the non-functional *phoP* gene (*phoP*$^-$) of YPIII was replaced by the functional *phoP*$^+$ gene of IP32953, yielding strain YP149 (YPIII *phoP*$^+$). Furthermore, the functional *phoP*$^+$ gene of IP32953 was exchanged by the mutated version of YPIII, yielding strain YPIP06 (IP32953 *phoP*$^-$).

Subsequently, RovA levels of the two sets of *phoP*$^{+}$ and *phoP*$^{-}$ strains were analyzed by western blotting at three different growth temperatures, leading to high (25°C), intermediate (32°C) and repressed (37°C) expression of RovA. As shown in Fig. **2**, the intracellular amount of RovA differed significantly between the *phoP*$^{+}$ and *phoP*$^{-}$ derivatives of IP32953 and YPIII at 32°C. At this growth temperature, RovA levels were considerably decreased in both *phoP*-negative strains. At 25°C, RovA levels were still markedly reduced in the *phoP*$^{-}$ derivative of IP32953, whereas similar levels of RovA were observed in the YPIII *phoP*$^{-}$ and its isogenic *phoP*$^{+}$ variant (Fig. **2**). RovA was not detectable at 37°C in any of the tested strains. This strongly indicated that PhoP acts as an activator of RovA expression in *Y. pseudotuberculosis* at moderate growth temperatures.

Activation of RovA expression by PhoP could occur directly or indirectly through other regulators, such as RovM, H-NS or the RovA-targeting proteases Lon and ClpP [35, 38, 39]. We addressed synthesis of the regulators in the *phoP*$^{+}$ and *phoP*$^{-}$ derivatives of YPIII and IP32953 and found that RovM levels were significantly increased in PhoP-deficient strains at 25°C, 32°C and 37°C (Fig. **2**). This strongly indicated that PhoP-dependent regulation of RovA expression in *Y. pseudotuberculosis* is mediated through downregulation of the transcriptional repressor RovM. Furthermore, we found that RovM levels were generally higher in IP32953 compared to YPIII (Fig. **2**), suggesting that not only PhoP, but also other regulatory components contribute to differential RovM levels.

PhoP-dependent expression of RovM is mediated via the small regulatory RNA CsrC

In previous studies we showed that synthesis of the LysR-type regulator RovM is controlled by the global regulator Crp and the Csr system in a nutrient-dependent

manner [30, 35, 40, 41]. To test whether PhoP-dependent regulation of RovM is linked to Crp and the Csr-system, we monitored expression of *crp* and *csrA* using translational *lacZ* fusions (Fig. **3A**,**B**), and compared the amounts of Crp and CsrA between the *phoP*$^+$ and *phoP*$^-$ derivatives of YPIII and IP32953. We did not observe any significant influence of PhoP on Crp and CsrA synthesis at 25°C and 37°C with both isolates (Fig. **3C**,**D**, Fig. **S1**).

Alternatively, it is possible that PhoP induces an upregulation of the CsrB and/or CsrC RNA, which both sequester and inhibit the function of CsrA, and this would lead in turn to a reduction of RovM synthesis (Fig. **1**,**2**). To determine whether PhoP acts on *Y. pseudotuberculosis* Csr RNAs we analyzed expression of *csrB*- and *csrC-lacZ* reporter fusions and performed northern blot experiments to compare CsrB and CsrC levels in the *phoP*$^+$ and *phoP*$^-$ derivatives of YPIII and IP32953 (Fig. **4**). In contrast to YPIII, CsrB is thermoregulated in IP32953 and highly expressed at 25°C, but not at 37°C (Fig. **4A-C**). Furthermore, CsrB synthesis was not affected in both strains by the absence of a functional *phoP* gene (Fig. **4A-C**). In contrast, *csrC* expression was significantly reduced in both *Y. pseudotuberculosis* strains lacking a functional *phoP* gene at 25°C and 37°C (Fig. **4D-F**). This indicated that the response regulator stimulates *csrC* transcription. The overall influence of PhoP on CsrC levels seemed much more pronounced in IP32953 as significantly lower amounts of the CsrC transcript were detectable in the *phoP*-deficient mutant of this isolate.

PhoP interacts with the *csrC* regulatory upstream region

In silico analysis identified two putative PhoP binding sites in the *csrC* regulatory region. One PhoP binding motif (position 61013-61030 of YPIII; NC_010465) is located 32 nucleotides upstream of the identified transcriptional start site (TSS) of *csrC* (position 61063) [40]. The second putative binding site is located more upstream at

197 position 60951-60968, i.e. 94 nucleotides upstream of the transcriptional start site.
198 Gel retardation assays were performed with increasing amounts of purified His-
199 tagged PhoP protein to test whether PhoP is able to interact directly and specifically
200 with the *csrC* regulatory region. DNA fragments encompassing different portions of
201 the *csrC* upstream region and a control fragment encoding the *gyrA* gene were
202 incubated with increasing concentrations of PhoP protein and assayed for protein-
203 DNA complex formation. As shown in Fig. **5A**, the PhoP protein interacted strongly in
204 a dose-dependent manner with the *csrC* regulatory region containing both putative
205 PhoP binding sites (-297 to +93), but no binding was detectable to the *gyrA* control
206 fragment. We further tested if PhoP binds to DNA fragments containing only one of
207 two predicted binding sites. PhoP interacted specifically and with a similar affinity
208 with both fragments (-297 to -55 and -76 to +93, relative to the transcriptional start
209 site at position 61063) (Fig. **5B**,**C**). This observation was confirmed by a competitive
210 gel retardation assay including both fragments of the *csrC* regulatory region with
211 single binding sites (Fig. **5D**).

212 To define the precise binding sites, DNase I footprinting experiments were per-
213 formed. The purified recombinant His-tagged PhoP protein protected two distinct
214 regions within the entire *csrC* regulatory region (Fig. **6**). The analysis of the antisense
215 and sense strand revealed two footprints, extending from -112 to -85 and -39 to -19
216 for the antisense strand, and from -18 to -49 and -85 to -112 for the sense strand,
217 overlapping the predicted binding sites. Binding of PhoP to the site closely upstream
218 of the TSS was less efficient, but could be improved by preincubation of purified
219 PhoP with acetyl phosphate. Within the protected regions two nucleotides became
220 hypersensitive towards DNase I in the presence of higher PhoP concentrations (Fig.
221 **6**). In summary, our data show that PhoP interacts directly and specifically with two
222 distinct sites located within the *csrC* regulatory region to stimulate *csrC* transcription.

223

224 **PhoP-dependent expression of *csrC* is initiated from two transcriptional start**
225 **sites**

226 Next, we analyzed whether PhoP-dependent *csrC* expression is initiated from the
227 promoter previously identified in our studies [40]. We mapped the 5'-ends of the CsrC
228 RNA and compared the amount of primer extension products in the *phoP*$^+$ and *phoP*$^-$
229 YPIII strain (Fig. **7A**). We selected YPIII for this analysis as in contrast to IP32953
230 CsrC was still detectable in the absence of *phoP* (Fig. **4E**). One transcriptional start
231 site (TSS 1) was mapped in both derivatives of YPIII, whereby the transcription level
232 from this site was much more enhanced in the YPIII *phoP*$^+$ derivative (Fig. **7A**). This
233 start site is identical with the transcriptional start site identified earlier at - strand
234 position 61063 [40]. Most strikingly, an additional start site (TSS 2) was located 61
235 nucleotides further upstream of TSS 1, which was more active in the YPIII *phoP*$^+$
236 derivative (YP149). A putative promoter sequence was identified closely upstream of
237 both transcriptional start sites, and each of the -35 regions of the promoters was
238 flanked by one PhoP box (Fig. **7B**). This indicates that PhoP activates expression of
239 CsrC from two distinct promoters, leading to a shorter and an extended CsrC
240 transcript. To verify the production of different CsrC species in the presence of PhoP,
241 we separated total RNA of the *phoP*$^+$ and *phoP*$^-$ derivatives of YPIII and IP32953 on
242 polyacrylamide gels to separate the predicted transcripts and performed northern blot
243 experiments. Two CsrC RNA species were detectable in both *Y. pseudotuberculosis*
244 strains in the presence of PhoP, but only the shorter CsrC transcript was visible in
245 YPIII harboring the non-functional PhoP allele (Fig. **7C**).

246

247 **Different stability of the CsrC transcripts in YPIII and IP32953**

Our comparative analysis of CsrC levels in this study has shown that the CsrC RNA was much less abundant in the *phoP*$^-$ derivative of IP32953 compared to YPIII harboring the identical *phoP* mutation (Fig. **4E**,**F**). Since the transcription of the *csrC-lacZ* fusion did not differ between the strains (Fig. **4D**), we hypothesized that the stability of the CsrC transcripts is reduced in IP32953.

Overall, the *csrC* locus is highly conserved between the *Y. pseudotuberculosis* strains YPIII and IP32953. However, an additional 20 nucleotides stretch is present within the *csrC* gene of IP32953, that is absent in YPIII and also not in *Y. pestis* CO92 (Fig. **S2**). Based on the repetitive DNA sequence it is likely that this variation is the result of two separate duplication events. To address whether this insertion has an influence on CsrC stability, we first determined the stability of $CsrC_{YPIII}$ and $CsrC_{IP32953}$ in strain YP149, harbouring a functional *phoP* gene ensuring maximal expression of the CsrC RNAs. As shown in Fig. **8**, the CsrC RNA of YPIII was slowly degraded with a half-life of about 90 min, whereas CsrC of IP32953 was less stable and decayed with a half-life of about 42 min. Furthermore, we integrated the additional 20 nucleotides stretch of the IP32953 CsrC RNA into CsrC of YPIII and tested the stability of the mutated transcript in the YPIII *phoP*$^+$ background (Fig. **8**). Degradation of the modified CsrC transcript was considerably enhanced. It decayed with a half-life similar to the IP32953 CsrC RNA, indicating that the insertion within CsrC promotes a more rapid degradation of this regulatory RNA in the *Y. pseudotuberculosis* wild-type strain IP32953.

Discussion

The ability of pathogenic bacteria to adjust their virulence-associated traits, physiological features and metabolic properties in response to the rapidly changing conditions within the host is crucial for a successful infection. Recently, it became evi-

dent that many invading bacteria use two-component systems to monitor nutritional, ion and physical changes and reprogram the expression of small regulatory RNAs of the post-transcriptional Csr/Rsm systems to manage virulence [41, 44]. In the related species *E. coli* and *Salmonella*, both Csr RNAs (CsrB and CsrC) are activated by the BarA/UvrY system at low pH and in the presence of weak organic acids [46, 47]. Moreover, all known Csr-type RNAs of *Legionella pneumophila, Pseudomonas aeruginosa* and *Vibrio cholerae* are induced by homologues of the BarA/UvrY system (LetS/LetA, VarS/VarA, and GacS/GacA). In *Yersinia* only CsrB is activated by BarA/UvrY [30, 40], whereas transcriptional regulators of *csrC* remained unknown.

In the present study, we show that the *Y. pseudotuberculosis* Csr system is also strongly regulated by the response regulator PhoP (Fig. **9**). Notably, an implication of the global Mg^{2+}-responsive two-component system PhoP/PhoQ system in the control of other Csr/Rsm systems has not previously been reported. PhoP induces transcription of the *csrC* gene, but not of *csrB*, by binding to two distinct PhoP box-like sequences within the *csrC* regulatory region. PhoP-dependent transcription of *csrC* starts from two independent start sites identified in close proximity of the identified PhoP binding sites. As a result, two small regulatory RNA species that differ 61 nucleotides in length are produced in the presence of PhoP, but not in the *phoP*-deficient strains. Whether the different transcripts vary in their function, e.g. in their capacity to bind CsrA is unclear. However, no additional potential CsrA binding sites (GGA motifs) are present in the added 5'-end of the extended CsrC transcript (Fig. **S2**). The formation of an additional hairpin structure, but no major changes of the overall CsrC structure were observed between the two variants as predicted by the Mfold software [48] (Fig. **S3**).

The molecular nature of the environmental stimuli controlling the Csr/Rsm systems in pathogens during infection is mostly unknown. However, a range of distinct in-

coming signals and participating regulators has been identified leading to a differential expression of the Csr-type RNAs. In *P. aeruginosa*, expression of both Rsm RNAs RsmY and RsmZ is differentially regulated through multiple sensor kinases and signaling pathways that converge to the GacA response regulator and control both sRNAs, or induce only the production of RsmY [49]. Moreover, the RsmY sRNA is more abundant than RsmZ, as the global H-NS family regulators MvaT and MvaU bind to an AT-rich motif in the upstream region of *rsmZ* to repress transcription, whereas *rsmY* is not affected [50, 51]. In *Y. pseudotuberculosis* the initial input comes from the independent two-component systems BarA/UvrY and PhoP/PhoQ, as well as Crp, which adjust the final output by a differential control of CsrB and CsrC levels according to the availability of nutrients and ions. The PhoP/PhoQ system responds to low Mg^{2+} and acidic pH frequently found within macrophages, and to various host-derived antimicrobial peptides that are part of the native immune response [52]. BarA/UvrY and Crp enable the bacteria to adjust to a switch of favoured catabolites (e.g. glucose) and an imbalance of TCA cycle intermediates (e.g. acetate, formate) [30, 46, 47]. These features underpin the possibility to fine-tune regulation of virulence determinants required to survive conditions experienced during extracellular and intracellular growth. There is evidence that *Y. pseudotuberculosis* is predominantly localized in extracellular sites during a systemic infection [53]. However, the bacteria can also multiply intracellular in professional phagocytes (e.g. macrophages) [45, 54]. This process is believed to be particularly important during the early stages of a systemic infection, in which the phagocytes appears to act as a trojan horse to reach deeper tissues. The phagocytes also function as a shelter for the pathogens to proliferate and induce pathogenicity determinants that enable them to annihilate the host immune response.

On the basis of this knowledge, it is likely that differences in the genetic equipment of the individual regulatory systems in different isolates of *Y. pseudotuberculosis* or in the closely related descendant *Y. pestis* determine distinct virulence properties. Here, we demonstrate that the expression of the Csr-type RNAs differs largely between the two *Y. pseudotuberculosis* isolates YPIII and IP32953. One reason is that *csrC* transcription in YPIII is reduced due to the absence of a functional *phoP* gene. Additionally, the stabilities of the CsrC RNAs are very different between the two *Y. pseudotuberculosis* strains, due to a 20 nucleotide insertion in the IP32953 CsrC RNA rendering the transcript much more susceptible to degradation (Fig. **9**). As a result, CsrC levels are significantly lower in a *phoP*$^-$ derivative of *Y. pseudotuberculosis* IP32953 compared to strain YPIII lacking a functional *phoP* allele. Differential regulation of Csr-type RNAs within *Y. pseudotuberculosis* is further supported by our finding that *csrB* expression is temperature-regulated in IP32953, but not in YPIII. The molecular basis for the different *csrB* expression pattern is still unknown, but it does not seem to require PhoP.

The different abundance of the Csr RNAs in YPIII and IP32953 contribute to varying levels of the virulence regulator RovA, inducing the expression of several virulence-associated traits, including the colonization factors InvA and PsaA [32, 33]. In YPIII, RovA is strongly expressed at moderate temperatures (25°C) despite the absence of PhoP, whereas in IP32953 PhoP is required to fully induce RovA expression. It seems feasible that enhanced RovA expression due to a stable CsrC RNA in YPIII allowed loss of a functional *phoP* gene, while the instable CsrC variant in IP32953 possibly demands presence of a functional *phoP* copy. A recent study revealed that PhoP also influences *rovA* expression in *Y. pestis* [28]. However, the regulation patterns seem considerably different from that observed in *Y. pseudotuberculosis*, which might indicate interesting evolutionary changes in the regulation of

crucial virulence factors between these species. Zhang *et al*. reported that PhoP inhibits transcription of *rovA* under Mg^{2+}-limiting conditions, but has no influence under Mg^{2+} rich or acidic pH conditions [28]. Under inducing conditions, PhoP recognizes a single site within the *rovA* regulatory region overlapping the transcriptional start site of promoter P1 [28]. Moreover, *Y. pestis* PhoP was shown to activate *crp* expression in rich medium [29]. However, in contrast to *Y. pestis*, PhoP does not affect *crp* expression and Crp levels in *Y. pseudotuberculosis* when cultured in rich medium. The species-specific differences are surprising, since the *crp, csrB, csrC* and the *rovA* promoter regions are highly conserved between *Y. pestis* and *Y. pseudotuberculosis* [55, 56], indicating that different regulator variants or other regulatory elements participate in the control of the Csr system in different yersiniae. This clearly illustrates that the regulatory networks controlled by the global regulators PhoP, Crp and CsrABC are tightly interwoven in order to control metabolism, host/-environmental adaptation and virulence in the genus *Yersinia*. However, the regulatory circuits and contributing components seem to vary greatly within and among *Yersinia* species suggesting that the Csr system is a focal point of global control to adapt the genus to different hosts and reservoirs.

In this context, it would also be interesting to know how the different outcomes of the PhoP-CsrABC-RovM-RovA regulatory cascade affect the infection process in the different *Yersinia* strains and species. Several studies demonstrated that the PhoP/PhoQ system is important for *Yersinia* virulence. It was shown in *in vitro* studies that *Y. pseudotuberculosis* and *Y. pestis* strains lacking the response regulator PhoP display an impaired survival and replication capacity inside macrophages and/or neutrophils [22, 45, 57, 58]. The role of PhoP for the virulence of both *Yersinia* species was also investigated by subcutaneous, aerosol and oral challenges of mice. However, the overall defect of the individual *phoP* mutants varied

377 significantly between different isolates of the two species. For instance, a 75-fold
378 higher LD_{50} has been determined for the *Y. pestis* strain GB mutated in *phoP* by
379 subcutaneous injections of mice (bubonic model) [22], whereas only a modest defect
380 was seen for a *phoP*$^-$ mutant of *Y. pestis* CO92 [24]. Furthermore, PhoP does not seem
381 to play a role for virulence of *Y. pestis* CO92 after an aerosol challenge (pneumonic
382 model) [24], but it is important for *Y. pseudotuberculosis* IP32953 and IP2666 during
383 aerosol infections [23, 24]. How PhoP and different levels of the Csr RNAs affect
384 virulence of YPIII and IP32953 after a natural oral challenge of mice is currently
385 unknown. One report describes that YPIII has a reduced ability to colonize lungs in a
386 systemic model in comparison to the *Y. pseudotuberculosis phoP*$^+$ strain IP2666 [23].
387 However, due to observed strain- and species-specific differences a more detailled
388 analysis comparing the regulatory circuits of PhoP and the Csr regulon in different *Y.*
389 *pestis* and *Y. pseudotuberculosis* strains with their impact on virulence is required to
390 fully understand how this regulatory node adapts individual yersiniae to different re-
391 servoirs and host niches.
392

393 ## Materials and Methods

394 **Bacterial strains, media and growth conditions**

395 The strains used in this work are listed in Table **1**. Bacteria were routinely grown in
396 Luria-Bertani (LB) broth to exponential growth phase (OD_{600nm} = 0.4-0.6) at 25°C,
397 32°C or 37°C under aerobic conditions. If necessary, antibiotics were added at the
398 following concentrations: carbenicillin 100 µg ml^{-1}, chloramphenicol 30 µg ml^{-1} and
399 kanamycin 50 µg ml^{-1}.
400

401 **DNA manipulation and plasmid construction analysis**

All DNA manipulations, restriction digestions, ligations and transformations were performed using standard genetic and molecular techniques [59, 60]. The plasmids used in this work are listed in Table **1**. Oligonucleotides used for PCR, sequencing and primer extension were purchased from Metabion and are listed in Table **2**. Plasmid DNA was isolated using Qiagen plasmid preparation kits. DNA-modifying enzymes and restriction enzymes were purchased from Roche or New England Biolabs. PCRs were done in a 100 µl mix for 29 cycles using *Taq* polymerase (Promega) or Phusion High-Fidelity DNA polymerase (New England Biolabs). Purification of PCR products was routinely performed using the QIAquick kit (Qiagen) or the Nucleic Acid and Protein Purification kit (Macherey Nagel). All constructed plasmids were sequenced by the in-house facility or GATC (Konstanz, Germany).

To generate plasmid pAKH103, the upstream regulatory region of *csrC* (-355 to +4) was amplified using primers 774 and I363 and cloned into the *Eco*RI/*Sal*I sites of pHT124. Plasmid pAKH139 carries a PCR generated fragment harboring the *crp* promoter region from nucleotide -491 (primer II432) to nucleotide +3 (primer II433) relative to the translational start. The fragment was digested and inserted into the *Xho*I/*Sal*I site of pFU67 resulting in a translational *crp-lacZ* fusion. The suicide mutagenesis plasmid pAKH188 was constructed by insertion of the additional 20 nucleotides of *csrC* of IP32953 into the *csrC* chromosomal sequence of YPIII. To do so, QuickChange mutagenesis (Stratagene) of pFS31 was performed using primers V604 and V605 according to the manufacturer's instructions. For the construction of plasmid pFS13, the entire *phoP* coding region (+1 to +671) was amplified from *Y. pseudotuberculosis* IP32953 with primers IV703 and IV704 and cloned into the *Bam*HI and *Hind*III sites of plasmid pET28a (Novagen). To generate plasmids pFS29 and pFS31, the *csrC*$^+$ fragments of *Y. pseudotuberculosis* strains IP32953 and YPIII were amplified by PCR using primers II850 and II853, digested with *Sac*I, and

428 inserted into the suicide mutagenesis plasmid pAKH3. To monitor *csrA* transcription,
429 the *csrA* promoter region (-1071) and 16 nucleotides of the coding region were
430 amplified by PCR using primers I617 and II275. The amplified fragment was
431 subsequently inserted into the *Pst*I site of pTS02 resulting in pKB63. For the
432 construction of plasmid pVP3, a kanamycin resistance cassette with 500 bp flanking
433 regions of the *phoPQ* locus was amplified with primer pair III925/III926 from
434 chromosomal DNA of YP56 and ligated into the *Sac*I/*Xho*I sites of pDM4. Plasmid
435 pWH1 was constructed by amplification of *phoPQ* of *Y. pseudotuberculosis* IP32953
436 with its 500 bp flanking regions using the primers III926 and III927. The fragment was
437 ligated into the *Sac*I/*Xho*I sites of pDM4.
438 Construction of a *csrC*-deficient derivative of the YPIII *phoPQ*$^+$ strain YP149 [61]
439 was performed by homologous recombination using suicide plasmid pAKH149 as
440 described previously [30]. The resulting strain YP285 was used for generation of strains
441 YP306, YP307 and YP308. The suicide plasmids pAKH188, pFS29 and pFS31 were
442 mated from S17-1λpir (*tra*$^+$) into YP285. Transconjugants were selected by plating on
443 *Yersinia* selective agar (Oxoid) supplemented with ampicillin. Subsequently, the
444 resulting strains were plated on LB plates containing 10% sucrose, which induces the
445 expression of the *sacB* gene on the integrated plasmid, leading to the production of a
446 toxic, growth-reducing substance. Fast growing colonies were selected to identify
447 clones in which the integrated plasmid including the wild-type copy of the target gene
448 was lost by a second spontaneous recombination process. The resulting strains were
449 tested for carbenicillin sensitivity and presence of the mutations was analyzed by
450 PCR and sequencing.
451 In order to generate *Y. pseudotuberculosis* IP32953 Δ*phoPQ* strain YPIP04, pVP3
452 was integrated into the *phoPQ* locus of strain IP32953 via conjugation as described
453 previously [34]. Chromosomal integration of the fragment was selected by plating the

bacteria on *Yersinia* selective agar supplemented with kanamycin. Conjugants with an excision of the plasmid including the functional *phoPQ* operon of IP32953 were identified after plating on 10% sucrose and selection of fast-growing, ampicillin sensitive strains as described above. Absence of the *phoPQ* operon was tested by PCR. To construct *Y. pseudotuberculosis* IP32953 *phoP*$^-$ strain YPIP06 harboring the non-functional *phoP* gene of YPIII, the plasmid pWH1 was conjugated into YPIP04. Chromosomal integration of the plasmid was selected by plating on *Yersinia* selective agar supplemented with chloramphenicol. The correct mutant was identified after plating on 10% sucrose as following: (i) fast-growing bacteria were isolated and tested for loss of the kanamycin cassette, (ii) presence of the *phoPQ* operon of YPIII was analyzed by PCR with primers III964, III965, III966, and III967, and (iii) presence of the *phoPQ* including the non-functional allele of *phoP* was confirmed by PCR and sequencing.

Expression and purification of the PhoP protein

E. coli strain BL21λDE3 pFS13 was grown at 37°C to exponential growth phase (OD_{600nm} = 0.4-0.6). Subsequently, the bacteria were shifted to 18°C and expression of His-tagged PhoP (His_6-PhoP) was induced with 1 mM IPTG (isopropyl-β-D-thiogalactoside). After 3 h bacteria were harvested by centrifugation (4°C, 20 min, 6.000-9.000 g) and resuspended in lysis buffer (50 mM NaH_2PO_4, 300 mM NaCl, 10 mM imidazol, pH 8.0). Bacterial cells were lysed with a French Press (Heinemann) and soluble His-PhoP protein was purified using a Ni-NTA agarose column (Macherey Nagel). The column was washed with four column volumes washing buffer (50 mM NaH_2PO_4, 300 mM NaCl, 20 mM imidazol, pH 8.0) and the His-tagged PhoP protein was eluted with elution buffer (50 mM NaH_2PO_4, 300 mM NaCl, 250 mM imidazol, pH 8.0). The purity of PhoP (>95%) was verified by SDS-PAGE.

480

481 **Electrophoretic mobility shift assay (EMSA)**

482 EMSAs were performed as described previously [35] with some modifications. For
483 DNA-binding studies three different fragments of the *csrC* upstream region were
484 amplified by PCR from genomic DNA of *Y. pseudotuberculosis* YPIII. One fragment
485 including both putative PhoP binding sites was amplified with primer pairs
486 IV937/IV939 (Table **2**). The other fragments harboring either PhoP binding site 1 or 2
487 were amplified with primer pairs IV938/IV939 and IV937/IV940, respectively. A
488 control fragment containing a part of the *gyrA* gene was amplified with primers
489 III186/III187. The purified PhoP protein was dialyzed against DNA-binding buffer (20
490 mM NaH_2PO_4, 100 mM KCl, 5% glycerol, 2 mM 1,4-dithiothreitol, pH 8.0). Equimolar
491 ratios of the DNA fragments and increasing amounts of PhoP were incubated in a 20
492 µl reaction mixture for 20 min at 25°C in DNA-binding buffer. The reaction mixture
493 was immediately loaded and separated on a 5% polyacrylamide gel, and stained with
494 ethidium bromide. The relative amount of unbound DNA was determined densio-
495 metrically using the software ImageJ (http://imagej.nih.gov/ij/) and the dissociation
496 constant (K_d) was calculated. The K_d values represent the mean ±SEM of three
497 independent experiments.

498

499 **DNase I footprinting**

500 The DNase I footprinting experiments were performed as described [35] with the
501 following modifications. First, the *csrC* promoter region was amplified from *Y.*
502 *pseudotuberculosis* YPIII using a sense digoxigenin (DIG)-labeled primer (I293) and
503 a non-labelled primer (I79), or an anti-sense digoxigenin (DIG)-labeled primer (V586)
504 and a non-labelled primer (V587). Either the His-tagged PhoP was used directly for
505 the footprint assay or the PhoP protein was phosphorylated by preincubation with 20

506 mM acetyl phosphate for 30 min at 25°C. The purified PCR product was incubated
507 with increasing amounts of His-tagged PhoP protein for 20 min in DNA-binding buffer
508 as described for the EMSA. The samples were treated with an appropriate dilution of
509 DNase I and stopped after 20 s by adding 50 µl stop solution (15 mM EDTA, 10 µg
510 ml^{-1} yeast carrier tRNA). The DNA was extracted by adding phenol-chloroform-
511 isoamylalcohol (25:24:1) and precipitated with ethanol. The samples were loaded on
512 a 6% polyacrylamide sequencing gel and run for 3 h at 60 W. The digested DNA
513 fragments were transferred on a Nytran membrane (GE Healthcare), UV crosslinked
514 and the protected DNA bands were detected using CDP-Star according to the DIG
515 Luminescent Detection kit (Roche). The DNA fragments used for the footprint reac-
516 tion were generated with the same DIG-labeled primer used for the amplification of
517 *csrC* for the sequencing reaction.
518 The sequencing reaction of the *csrC* upstream region was performed using the
519 dideoxy-chain reaction with the Thermo Sequenase cycle sequencing kit (Affymetrix)
520 according to the manufacturer's instructions. The *csrC* upstream region was
521 amplified from the plasmid pAKH59 with the digoxigenin (DIG)-labeled sense primer
522 I293 or the anti-sense primer V586.
523
524 **Primer extension analysis**
525 Primer extension analysis was performed as described previously [35] with minor
526 modifications. Total RNA was isolated using the hot phenol method and 20 µg of total
527 RNA were reverse transcribed using the digoxigenin-labelled primer I293 specific for
528 the *csrC* gene. The sequencing reaction was carried out with primer I293 as
529 described for DNase I footprinting.
530
531 **Western blotting**

For the detection of the regulatory proteins RovA, RovM, Crp and CsrA, cultures of the *Y. pseudotuberculosis* strains were grown under specific environmental conditions as described. Bacterial whole cell extracts were prepared from equal amounts of bacteria and separated on SDS-polyacrylamide gels, and blotted onto nitrocellulose membranes [60]. Subsequently, membranes were blocked in 1 x TBST containing 3% BSA (blocking buffer). Primary, polyclonal rabbit IgG antibodies (anti-RovA, anti-RovM, anti-Crp and anti-CsrA) were added in a 1:4.000 dilution in blocking buffer. The secondary antibody, anti-rabbit IgG conjugated with horse radish peroxidase, was supplied in a 1:8.000 dilution in blocking buffer and the immunological detection of the proteins was performed as described previously [30, 40]. Relative protein amounts were determined densiometrically using the software ImageJ (http://imagej.nih.gov/ij/) for three independent experiments and normalized to the respective unspecific protein band. Statistical analysis was performed by student´s t test.

RNA isolation, Northern blotting and RNA stability assays

For the isolation of total RNA, exponentially grown cultures of *Y. pseudotuberculosis* strains were cultivated at 25°C or 37°C. Bacterial cells were harvested by centrifugation (10.000 g) at the same temperature as the respective experiment was performed, and the cell pellet was snap-frozen in liquid nitrogen. Total RNA from the samples was isolated by the hot phenol method [30], and quantified photometrically using a wavelength of 260 nm.

For northern blotting total RNA (5 µg) was mixed with loading buffer (0.03% bromophenol blue, 4 mM EDTA, 0.1 mg/ml EtBr, 2.7% formaldehyde, 31% formamide, 20% glycerol in 4 x MOPS buffer), heated for 10 min at 70°C, separated on MOPS agarose gels (1,2%) and transferred by vacuum blotting for 1,5 h onto positively

charged membranes (GE Healthcare) in 10 x SSC. To detect the two different transcripts of CsrC high-resolution gels (urea acrylamide, 12%) were performed. Total RNA (10 µg) was separated for 3 h at 140 V and transferred onto positively charged membranes (GE Healthcare) in 0,5 x TBE for 30 min at 20 V using semi-dry blotting system. The membrane was UV cross-linked. DIG-labeled *csrB* and *csrC* PCR-fragments were amplified with primer pairs 555/556 and 582/583 respectively (Table **2**) using the DIG-PCR nucleotide mix (Roche). Prehybridization (1-2 h, 42°C), hybridization (overnight, 42°C) and washing were conducted using the DIG Luminescent Detection kit (Roche) according to the manufactures instructions.

RNA stability assay was used to compare degradation of the different CsrC RNAs. Exponentially grown cultures of bacteria expressing the different CsrC variants were mixed with rifampicin (2 mg/ml) to inhibit transcription. At certain time points after blockage of transcription, samples were withdrawn, mixed with 0,2 volume of stop solution (5% water-saturated phenol, 95% ethanol) and snap-frozen in liquid nitrogen. The pellets were thawed on ice, centrifugated (4°C, 10 min, 14.000 rpm) and RNA was isolated using the SV total RNA purification kit (Promega) as described by the manufacturer. Separation and detection of the RNA were performed as described above. The half-life of CsrC was calculated by least squares analysis of semi-logarithmic plots of CsrC RNA amounts, normalized to 23S and 16S rRNA, versus time.

Analysis of reporter gene expression

The β-galactosidase activity of the *lacZ* fusion constructs was measured in permeabilized cells as described previously [34]. The activity was calculated as follows: β-galactosidase activity $OD_{420nm} * 6{,}648^{-1} * OD_{600nm}^{-1} * t\ (min)^{-1} * Vol\ (ml)^{-1}$.

Acknowledgements

584 We thank Dr. Martin Fenner for helpful and motivating discussions. We also thank
585 Katja Böhme and Verena Pianka for plasmids, and Tanja Krause, Sandra Stengel
586 and Karin Paduch for experimental support. This work was supported by the Deut-
587 sche Forschungsgemeinschaft Grants DE616/3-2 (SPP1258) for PD and AKH,
588 DE616/4-2 (SPP1316) for AN, and DE616/5-1 (SPP1617) for FS, a stipend of the
589 HZI Graduate School for WH, the Deutsche Zentrum für Infektionsforschung (DZIF)
590 for FP and PD, and the Fonds der Chemischen Industrie for PD.
591

592 ## References

593 1. Stock AM, Robinson VL, Goudreau PN. Two-component signal transduction.
594 Annu Rev Biochem 2000; 69:183-215.
595 2. Gao R, Stock AM. Biological insights from structures of two-component proteins.
596 Annu Rev Microbiol 2009; 63:133-54.
597 3. Mascher T, Helmann JD, Unden G. Stimulus perception in bacterial signal-
598 transducing histidine kinases. Microbiol Mol Biol Rev 2006; 70:910-38.
599 4. Groisman EA. The pleiotropic two-component regulatory system PhoP-PhoQ. J
600 Bacteriol 2001; 183:1835-42.
601 5. Gooderham WJ, Hancock RE. Regulation of virulence and antibiotic resistance
602 by two-component regulatory systems in *Pseudomonas aeruginosa*. FEMS
603 Microbiol Rev 2009; 33:279-94.
604 6. Brodsky IE, Gunn JS. A bacterial sensory system that activates resistance to
605 innate immune defenses: potential targets for antimicrobial therapeutics. Mol
606 Interv 2005; 5:335-7.
607 7. Kato A, Tanabe H, Utsumi R. Molecular characterization of the PhoP-PhoQ two-
608 component system in *Escherichia coli* K-12: identification of extracellular Mg2+-
609 responsive promoters. J Bacteriol 1999; 181:5516-20.

8. Soncini FC, Vescovi EG, Groisman EA. Transcriptional autoregulation of the *Salmonella typhimurium phoPQ* operon. J Bacteriol 1995; 177:4364-71.
9. Li Y, Gao H, Qin L, Li B, Han Y, Guo Z, et al. Identification and characterization of PhoP regulon members in *Yersinia pestis* biovar Microtus. BMC Genomics 2008; 9:143.
10. Minagawa S, Ogasawara H, Kato A, Yamamoto K, Eguchi Y, Oshima T, et al. Identification and molecular characterization of the Mg2+ stimulon of *Escherichia coli*. J Bacteriol 2003; 185:3696-702.
11. Yamamoto K, Ogasawara H, Fujita N, Utsumi R, Ishihama A. Novel mode of transcription regulation of divergently overlapping promoters by PhoP, the regulator of two-component system sensing external magnesium availability. Mol Microbiol 2002; 45:423-38.
12. Lejona S, Aguirre A, Cabeza ML, Garcia Vescovi E, Soncini FC. Molecular characterization of the Mg2+-responsive PhoP-PhoQ regulon in *Salmonella enterica*. J Bacteriol 2003; 185:6287-94.
13. Fields PI, Swanson RV, Haidaris CG, Heffron F. Mutants of *Salmonella typhimurium* that cannot survive within the macrophage are avirulent. Proc Natl Acad Sci U S A 1986; 83:5189-93.
14. Miller SI, Kukral AM, Mekalanos JJ. A two-component regulatory system (*phoP phoQ*) controls *Salmonella typhimurium* virulence. Proc Natl Acad Sci U S A 1989; 86:5054-8.
15. Oyston PC, Dorrell N, Williams K, Li SR, Green M, Titball RW, et al. The response regulator PhoP is important for survival under conditions of macrophage-induced stress and virulence in *Yersinia pestis*. Infect Immun 2000; 68:3419-25.

16. Grabenstein JP, Fukuto HS, Palmer LE, Bliska JB. Characterization of phagosome trafficking and identification of PhoP-regulated genes important for survival of *Yersinia pestis* in macrophages. Infect Immun 2006; 74:3727-41.
17. O'Loughlin JL, Spinner JL, Minnich SA, Kobayashi SD. *Yersinia pestis* two-component gene regulatory systems promote survival in human neutrophils. Infect Immun 2010; 78:773-82.
18. Hitchen PG, Prior JL, Oyston PC, Panico M, Wren BW, Titball RW, et al. Structural characterization of lipo-oligosaccharide (LOS) from Yersinia pestis: regulation of LOS structure by the PhoPQ system. Mol Microbiol 2002; 44:1637-50.
19. Fields PI, Groisman EA, Heffron F. A *Salmonella* locus that controls resistance to microbicidal proteins from phagocytic cells. Science 1989; 243:1059-62.
20. Galan JE, Curtiss R, 3rd. Virulence and vaccine potential of *phoP* mutants of *Salmonella typhimurium*. Microb Pathog 1989; 6:433-43.
21. Bozue J, Mou S, Moody KL, Cote CK, Trevino S, Fritz D, et al. The role of the *phoPQ* operon in the pathogenesis of the fully virulent CO92 strain of *Yersinia pestis* and the IP32953 strain of *Yersinia pseudotuberculosis*. Microb Pathog 2011; 50:314-21.
22. Oyston PC, Dorrell N, Williams K, Li SR, Green M, Titball RW, et al. The response regulator PhoP is important for survival under conditions of macrophage-induced stress and virulence in *Yersinia pestis*. Infect Immun 2000; 68:3419-25.
23. Fisher ML, Castillo C, Mecsas J. Intranasal inoculation of mice with *Yersinia pseudotuberculosis* causes a lethal lung infection that is dependent on *Yersinia* outer proteins and PhoP. Infect Immun 2007; 75:429-42.

660 24. Bozue J, Mou S, Moody KL, Cote CK, Trevino S, Fritz D, et al. The role of the
661 *phoPQ* operon in the pathogenesis of the fully virulent CO92 strain of *Yersinia*
662 *pestis* and the IP32953 strain of *Yersinia pseudotuberculosis*. Microb Pathog
663 2011; 50:314-21.
664 25. Perez JC, Groisman EA. Transcription factor function and promoter architecture
665 govern the evolution of bacterial regulons. Proc Natl Acad Sci U S A 2009;
666 106:4319-24.
667 26. Perez JC, Shin D, Zwir I, Latifi T, Hadley TJ, Groisman EA. Evolution of a
668 bacterial regulon controlling virulence and Mg(2+) homeostasis. PLoS Genet
669 2009; 5:e1000428.
670 27. Zhou D, Han Y, Qin L, Chen Z, Qiu J, Song Y, et al. Transcriptome analysis of
671 the Mg2+-responsive PhoP regulator in *Yersinia pestis*. FEMS Microbiol Lett
672 2005; 250:85-95.
673 28. Zhang Y, Gao H, Wang L, Xiao X, Tan Y, Guo Z, et al. Molecular characterization
674 of transcriptional regulation of *rovA* by PhoP and RovA in *Yersinia pestis*. PLoS
675 One 2011; 6:e25484.
676 29. Zhang Y, Wang L, Han Y, Yan Y, Tan Y, Zhou L, et al. Autoregulation of
677 PhoP/PhoQ and positive regulation of the cyclic AMP receptor protein-cyclic
678 AMP complex by PhoP in *Yersinia pestis*. J Bacteriol 2013; 195:1022-30.
679 30. Heroven AK, Sest M, Pisano F, Scheb-Wetzel M, Steinmann R, Bohme K, et al.
680 Crp induces switching of the CsrB and CsrC RNAs in *Yersinia*
681 *pseudotuberculosis* and links nutritional status to virulence. Front Cell Infect
682 Microbiol 2012; 2:158.
683 31. Ellison DW, Miller VL. Regulation of virulence by members of the MarR/SlyA
684 family. Curr Opin Microbiol 2006; 9:153-9.

685 32. Cathelyn JS, Ellison DW, Hinchliffe SJ, Wren BW, Miller VL. The RovA regulons
686 of *Yersinia enterocolitica* and *Yersinia pestis* are distinct: evidence that many
687 RovA-regulated genes were acquired more recently than the core genome. Mol
688 Microbiol 2007; 66:189-205.
689 33. Cathelyn JS, Crosby SD, Lathem WW, Goldman WE, Miller VL. RovA, a global
690 regulator of *Yersinia pestis*, specifically required for bubonic plague. Proc Natl
691 Acad Sci U S A 2006; 103:13514-9.
692 34. Nagel G, Lahrz A, Dersch P. Environmental control of invasin expression in
693 *Yersinia pseudotuberculosis* is mediated by regulation of RovA, a transcriptional
694 activator of the SlyA/Hor family. Mol Microbiol 2001; 41:1249-69.
695 35. Heroven AK, Dersch P. RovM, a novel LysR-type regulator of the virulence
696 activator gene *rovA*, controls cell invasion, virulence and motility of *Yersinia*
697 *pseudotuberculosis*. Mol Microbiol 2006; 62:1469-83.
698 36. Dube PH, Handley SA, Revell PA, Miller VL. The *rovA* mutant of *Yersinia*
699 *enterocolitica* displays differential degrees of virulence depending on the route of
700 infection. Infect Immun 2003; 71:3512-20.
701 37. Revell PA, Miller VL. A chromosomally encoded regulator is required for
702 expression of the *Yersinia enterocolitica inv* gene and for virulence. Mol Microbiol
703 2000; 35:677-85.
704 38. Heroven A, Nagel G, Tran HJ, Parr S, Dersch P. RovA is autoregulated and
705 antagonizes H-NS-mediated silencing of invasin and *rovA* expression in *Yersinia*
706 *pseudotuberculosis*. Mol Microbiol 2004; 53:871-88.
707 39. Herbst K, Bujara M, Heroven AK, Opitz W, Weichert M, Zimmermann A, et al.
708 Intrinsic thermal sensing controls proteolysis of *Yersinia* virulence regulator
709 RovA. PLoS Pathog 2009; 5:e1000435.

710 40. Heroven A, Bohme K, Rohde M, Dersch P. A Csr-type regulatory system,
711 including small non-coding RNAs, regulates the global virulence regulator RovA
712 of *Yersinia pseudotuberculosis* through RovM. Mol Microbiol 2008; 68:1179-95.
713 41. Heroven AK, Bohme K, Dersch P. The Csr/Rsm system of *Yersinia* and related
714 pathogens: A post-transcriptional strategy for managing virulence. RNA Biol
715 2012; 9.
716 42. Romeo T, Vakulskas CA, Babitzke P. Post-transcriptional regulation on a global
717 scale: form and function of Csr/Rsm systems. Environ Microbiol 2012.
718 43. Babitzke P, Romeo T. CsrB sRNA family: sequestration of RNA-binding
719 regulatory proteins. Curr Opin Microbiol 2007; 10:156-63.
720 44. Timmermans J, Van Melderen L. Post-transcriptional global regulation by CsrA in
721 bacteria. Cell Mol Life Sci 2010; 67:2897-908.
722 45. Grabenstein JP, Marceau M, Pujol C, Simonet M, Bliska JB. The response
723 regulator PhoP of *Yersinia pseudotuberculosis* is important for replication in
724 macrophages and for virulence. Infect Immun 2004; 72:4973-84.
725 46. Chavez RG, Alvarez AF, Romeo T, Georgellis D. The physiological stimulus for
726 the BarA sensor kinase. J Bacteriol 2010; 192:2009-12.
727 47. Mondragon V, Franco B, Jonas K, Suzuki K, Romeo T, Melefors O, et al. pH-
728 dependent activation of the BarA-UvrY two-component system in *Escherichia*
729 *coli*. J Bacteriol 2006; 188:8303-6.
730 48. Zuker M. Mfold web server for nucleic acid folding and hybridization prediction.
731 Nucleic Acids Res 2003; 31:3406-15.
732 49. Bordi C, Lamy MC, Ventre I, Termine E, Hachani A, Fillet S, et al. Regulatory
733 RNAs and the HptB/RetS signalling pathways fine-tune *Pseudomonas*
734 *aeruginosa* pathogenesis. Mol Microbiol 2010; 76:1427-43.

735 50. Brencic A, Lory S. Determination of the regulon and identification of novel mRNA
736 targets of *Pseudomonas aeruginosa* RsmA. Mol Microbiol 2009; 72:612-32.
737 51. Brencic A, McFarland KA, McManus HR, Castang S, Mogno I, Dove SL, et al.
738 The GacS/GacA signal transduction system of *Pseudomonas aeruginosa* acts
739 exclusively through its control over the transcription of the RsmY and RsmZ
740 regulatory small RNAs. Mol Microbiol 2009; 73:434-45.
741 52. Groisman EA, Mouslim C. Sensing by bacterial regulatory systems in host and
742 non-host environments. Nat Rev Microbiol 2006; 4:705-9.
743 53. Simonet M, Richard S, Berche P. Electron microscopic evidence for *in vivo*
744 extracellular localization of *Yersinia pseudotuberculosis* harboring the pYV
745 plasmid. Infect Immun 1990; 58:841-5.
746 54. Pujol C, Bliska JB. The ability to replicate in macrophages is conserved between
747 *Yersinia pestis* and *Yersinia pseudotuberculosis*. Infect Immun 2003; 71:5892-9.
748 55. Parkhill J, Wren BW, Thomson NR, Titball RW, Holden MT, Prentice MB, et al.
749 Genome sequence of *Yersinia pestis*, the causative agent of plague. Nature
750 2001; 413:523-7.
751 56. Song Y, Tong Z, Wang J, Wang L, Guo Z, Han Y, et al. Complete genome
752 sequence of *Yersinia pestis* strain 91001, an isolate avirulent to humans. DNA
753 Res 2004; 11:179-97.
754 57. Grabenstein JP, Fukuto HS, Palmer LE, Bliska JB. Characterization of
755 phagosome trafficking and identification of PhoP-regulated genes important for
756 survival of *Yersinia pestis* in macrophages. Infect Immun 2006; 74:3727-41.
757 58. O'Loughlin JL, Spinner JL, Minnich SA, Kobayashi SD. *Yersinia pestis* two-
758 component gene regulatory systems promote survival in human neutrophils.
759 Infect Immun 2010; 78:773-82.

760 59. Miller JH. A short course in bacterial genetic: a laboratory manual and handbook
761 for *Escherichia coli* and related bacteria. Cold Spring Habor, New York, 1992.
762 60. Sambrook J. Molecular Cloning: A Laboratory Manual,. Cold Spring Harbor
763 Laboratories, Cold Spring Harbor, NY, 2001.
764 61. Schweer J, Kulkarni D, Kochut A, Pezoldt J, Pisano F, Pils MC, et al. The
765 cytotoxic necrotizing factor of *Yersinia pseudotuberculosis* (CNFY) enhances
766 inflammation and Yop delivery during infection by activation of Rho GTPases.
767 PLoS Pathog 2013; 9:e1003746.
768
769

Figure legends

Figure 1. Regulatory cascade controlling expression of *Y. pseudotuberculosis* early-stage virulence genes. Expression of the virulence genes invasin (*invA*) and *psaA* is activated by the thermosensing virulence regulator RovA. Synthesis of RovA is controlled in a nutrient-dependent manner by a regulatory cascade, including the cAMP receptor protein (Crp) and the two-component regulatory proteins UvrY/BarA. They regulate components of the carbon storage regulator (Csr) system, i.e. the regulatory RNAs CsrB and CsrC and the RNA-binding protein CsrA. Upregulation of CsrB and/or CsrC leads to the sequestration of CsrA, whereby synthesis of the LysR-type repressor RovM is inhibited, which allows production of RovA. Furthermore, RovM synthesis is repressed by Crp downstream of CsrA via an unknown mechanism. The new finding that *csrC* expression is activated by the PhoP/PhoQ two component system is highlighted in red. Solid lines illustrate direct control, and dashed lines indirect regulation by the indicated regulator.

Figure 2. PhoP-dependent RovA expression is mediated via RovM. Whole cell extracts of YPIII (*phoP*$^-$), YP149 (YPIII *phoP*$^+$), IP32953 (*phoP*$^+$) and YPIP06 (IP32953 *phoP*$^-$) grown to exponential phase at 25°C, 32°C and 37°C were separated by SDS-PAGE prior to western blotting using polyclonal RovA- and RovM-specific antibodies. As negative controls *rovA* and *rovM* deletion strains YP107 and YP72 were included. Relative protein amounts were determined densiometrically using the software ImageJ for three independent experiments and normalized to the respective unspecific protein band (c). Statistical analysis was performed by student´s t test with * (P≤0.05), ** (P≤0.005), *** (P≤0.001), n.s. (not significant) and n.d. (not detectable).

796

797 **Figure 3.** Analysis of *crp* and *csrA* expression in *phoP*$^+$ and *phoP*$^-$ strains. The vector
798 pAKH139, harboring a *crp-lacZ* fusion **(A)** and plasmid pKB63, harboring a *csrA-lacZ*
799 fusion **(B)** were transformed into *Y. pseudotuberculosis* strains YPIII (*phoP*$^-$), YP149
800 (YPIII *phoP*$^+$), IP32953 (*phoP*$^+$) and YPIP06 (IP32953 *phoP*$^-$). The bacteria were
801 grown to exponential growth phase in LB medium at 25°C. The data represent the
802 mean ±SEM from three independent experiments each performed in triplicates.
803 Whole cell extracts of YPIII (*phoP*$^-$), YP149 (YPIII *phoP*$^+$), IP32953 (*phoP*$^+$) and
804 YPIP06 (IP32953 *phoP*$^-$) grown to exponential growth phase at 25°C were separated
805 by SDS-PAGE prior to western blotting using polyclonal Crp- **(C)** and CsrA- **(D)**
806 specific antibodies. As negative controls *crp* and *csrA* deletion strains YP89 and
807 YP53 were included. Relative protein amounts were determined densiometrically
808 using the software ImageJ for three independent experiments and normalized to the
809 respective unspecific protein band (c). Statistical analysis was performed by
810 student´s t test with * (P≤0.05), ** (P≤0.005), *** (P≤0.001), n.s. (not significant) and
811 n.d. (not detectable).
812

813 **Figure 4.** Influence of PhoP on CsrB and CsrC synthesis. The vector pAKH101,
814 harboring a *csrB-lacZ* fusion (**A**), and the vector pAKH103, harboring a *csrC-lacZ*
815 fusion (**D**), were transformed into *Y. pseudotuberculosis* strains YPIII (*phoP*$^-$), YP149
816 (YPIII *phoP*$^+$), IP32953 (*phoP*$^+$) and YPIP06 (IP32953 *phoP*$^-$). The cells were grown
817 to exponential growth phase in LB medium at 25°C. The data represent the mean
818 ±SEM from at least two different experiments each done in triplicate and were
819 analyzed with Student's t-test. ***: P<0,001. Total RNA from *Y. pseudotuberculosis*
820 strains YPIII (*phoP*$^-$), YP149 (YPIII *phoP*$^+$), IP32953 (*phoP*$^+$) and YPIP06 (IP32953
821 *phoP*$^-$) grown to exponential growth phase at 25°C (**B**,**E**) or 37°C (**C**,**F**) was prepared

822 and analyzed by northern blotting with CsrB (**B**,**C**) and CsrC (**E**,**F**) specific probes.
823 YPIII *ΔcsrB* and YPIII *ΔcsrC* served as negative control, respectively.
824
825 **Figure 5.** Interaction of PhoP with the *csrC* promoter region. Three different DNA
826 promoter fragments of *csrC* were incubated with increasing concentrations of PhoP.
827 A *gyrA* fragment was used as negative control (c). The PhoP-DNA complexes were
828 separated on 5% polyacrylamide gels. The position of the specific higher molecular
829 weight DNA-protein complexes is marked with an asterisk. The analyzed fragments
830 were the following: *csrC* 1 (-297 to +93) **(A)**, *csrC* 2 (-297 to -55) **(B)**, *csrC* 3 (-76 to
831 +93) **(C)** and *csrC* 2 (-297 to -55) competitive with *csrC* 3 (-76 to +93) **(D)**. The
832 relative amount of unbound DNA was determined densiometrically using the software
833 ImageJ and the dissociation constant (K_d) was calculated. The K_d values represent
834 the mean ± SEM of three independent experiments.
835
836 **Figure 6.** DNase I footprinting of PhoP with the *csrC* regulatory region. Sense (**A**)
837 and antisense (**B**) *csrC*-probes were DIG-labeled and incubated with increasing
838 amounts of purified His-PhoP or His-PhoP preincubated with acetyl phosphate. DNA
839 or PhoP-DNA complexes were digested with DNase I and separated on a 6%
840 polyacrylamide gel. Lanes T, C, A, G represent the Sanger sequencing reactions.
841 The DNase I protected regions are indicated with vertical bars, hypersensitive
842 regions are marked with an asterisk. The numbers indicate the nucleotide positions
843 upstream of *csrC*.
844
845 **Figure 7.** PhoP-dependent transcription of *csrC* occurs from two distinct start sites.
846 **(A)** Mapping of the *csrC* transcriptional start site. For primer extension of the CsrC
847 transcript total RNA isolated from YPIII and YP149 (YPIII *phoP*$^+$) grown at 25°C in

LB, and a Dig-labeled *csrC* specific primer was used. The sequencing reaction (left site) was performed with the same primer used for the extension reaction. The transcriptional start sites (TSSs) are indicated by arrows. **(B)** Regulatory region of *csrC*, illustrating the two putative promoters, the identified transcriptional start sites, the DNase I protected areas (highlighted in grey) and putative PhoP boxes (bold letters). **(C)** High-resolution northern blot of CsrC revealing two CsrC isoforms. Total RNA was isolated from YPIII (*phoP*$^-$) and YP149 (YPIII *phoP*$^+$) as well as IP32953 (*phoP*$^+$) and YPIP06 (IP32953 *phoP*$^-$) grown to exponential growth phase at 25°C in LB. 10 µg of RNA were separated using urea-acrylamide gels and analyzed by northern blotting with CsrC specific probes. YPIII *ΔcsrC* served as negative control.

Figure 8. RNA stability assay of CsrC. **(A)** A RNA stability assay of CsrC in the three different strains YP308 ($CsrC_{YPIII}$), YP307 ($CsrC_{IP32953}$) and YP306 ($CsrC_{YPIII+20nt\ IP32953}$) was performed. RNA synthesis was stopped by adding 2 mg/ml rifampicin and samples were taken after 0, 15, 30, 45, 60, 90 and 120 min. **(B)** The half-life of CsrC was measured by a least squares analysis of semi-logarithmic plots of RNA concentration versus time and represent the mean ±SEM from three different experiments.

Figure 9. Model of PhoP-dependent regulation of *csrC* transcription. The current model displays PhoP-dependent regulation of *csrC* expression and derivative-specific differences in CsrC transcript stability in *Y. pseudotuberculosis* YPIII and IP32953. Expression of *csrC* is positively regulated by PhoP via direct DNA-interaction. PhoP stimulates *csrC* expression from two distinct promoters resulting in two CsrC isoforms. IP32953 CsrC carries an additional 20 nucleotides stretch (black box) leading to decreased CsrC stability.

Supplements

Figure S1. Analysis of *crp* and *csrA* expression in *phoP*$^+$ and *phoP*$^-$ strains. The vector pAKH139, harboring a *crp-lacZ* fusion **(A)** and plasmid pKB63, harboring a *csrA-lacZ* fusion **(B)** were transformed into *Y. pseudotuberculosis* strains YPIII (*phoP*$^+$), YP149 (YPIII *phoP*$^+$), IP32953 (*phoP*$^+$) and YPIP06 (IP32953 *phoP*$^-$). The bacteria were grown to exponential growth phase in LB medium at 37°C. The data represent the mean ±SEM from three independent experiments each performed in triplicates. Whole cell extracts of YPIII (*phoP*$^-$), YP149 (YPIII *phoP*$^+$), IP32953 (*phoP*$^+$) and YPIP06 (IP32953 *phoP*$^-$) grown to exponential growth phase at 37°C were separated by SDS-PAGE prior to western blotting using polyclonal Crp- **(C)** and CsrA- **(D)** specific antibodies. As negative controls *crp* and *csrA* deletion strains YP89 and YP53 were included. Relative protein amounts were determined densiometrically using the software ImageJ for three independent experiments and normalized to the respective unspecific protein band (c). Statistical analysis was performed by student´s t test with * (P≤0.05), ** (P≤0.005), *** (P≤0.001) and n.s. (not significant).

Figure S2. Sequence alignment of *csrC* of *Y. pseudotuberculosis* and *Y. pestis* strains. ClustalW alignment of *csrC* sequences from *Yersinia* species. The nucleotide sequences of *csrC* of *Y. pseudotuberculosis* strains YPIII (accession no. NC_010465.1), IP32953 (accession no. NC_006155.1), IP31758 (accession no. NC_009708.1), PB1/+ (accession no. NC_010634.1), and *Y. pestis* strains CO92 (accession no. NC_003143.1) and biovar Microtus 91001 (accession no. NC_005810.1). The *csrC* DNA sequence selected for the alignment starts at the second transcriptional start site identified in this study and covers the entire anno-

900 tated *csrC* gene. The red and yellow marked sequences indicate the additional
901 repetitive nucleotides in the *csrC* sequence of IP32953 which were most likely
902 acquired due to rearrangements including nucleotides 125-144.
903
904 **Figure S3.** RNA secondary structure prediction of YPIII short and extended CsrC
905 variants. The secondary structures of CsrC starting from TSS 1 (short variant) (**A**) or
906 TSS 2 (extented variant) (**B**) were predicted by using the Mfold software [48]. The
907 extended stretch ranging from TSS 1 to TSS 2 is highlighted.

Table 1: Bacterial strains and plasmids.

Strains, plasmids	Description	Source and reference
Bacterial strains		
E. coli K-12		
BL21λDE3	F$^-$ *ompT gal dcm lon hsdSB (rB2 mB2) gal* λDE3	[55]
S17-1λpir	*recA1 thi pro hsdR*$^-$ RP4-2Tc::Mu Km::Tn7 λpir	[56]
Y. pseudotuberculosis		
IP32953	pIB1, wild-type	[57]
YPIII	pYV, wild-type	[58]
YP53	YPIII, Δ*csrA*, Kn^R	[40]
YP56	YPIII, Δ*phoPQ*, Kn^R	[54]
YP69	YPIII, Δ*csrB*	[40]
YP72	YPIII, Δ*rovM*	Heroven *et al.*, 2012
YP89	YPIII, Δ*crp*, Kn^R	[30]
YP107	YPIII, Δ*rovA*	Quade *et al.*, 2012
YP126	YPIII, Δ*csrC*	[30]
YP149	YPIII, *phoPQ*^{IP32953}	[54]
YP285	YP149, Δ*csrC*, Kn^R	This study
YP306	YP285, *csrC*$_{YPIII20nt\ IP32953}$	This study
YP307	YP285, *csrC*$_{IP32953}$	This study
YP308	YP285, *csrC*$_{YPIII}$	This study
YPIP04	IP32953, Δ*phoPQ*, Kn^R	This study
YPIP06	IP32953, *phoPQ*^{YPIII}	This study
Plasmids		
pACYC184	Cloning vector, Tet^R, Cm^R	[59]
pAKH3	pGP704, *sacB*$^+$, Ap^R	[30]
pAKH59	pACYC184, *csrC*$^+$, Cm^R	[40]
pAKH101	pHT124, *csrB-lacZ*(4)^a, Ap^R	[40]
pAKH103	pHT124, *csrC-lacZ*(4)^a, Ap^R	This study
pAKH139	pFU67, *crp-lacZ*(1)^b, Ap^R	This study
pAKH149	pAKH3, *csrC*::Kan^R	[30]
pAKH188	pFS31, *csrC*$_{YPIII20nt\ IP32953}$	This study
pDM4	R6K derivate, *sacB*, Cm^R	[60]
pFS13	pET28a, *phoP*$^+$, Kn^R	This study
pFS29	pAKH3, *csrC*$_{IP32953}$	This study

pFS31	pAKH3, *csrC*$_{YPIII}$	This study
pFU67	promoterless *lacZ*, ori pSC101*, Cm^R	[61]
pHT124	promoter-probe vector, *lacZ*$^+$, Ap^R	[40]
pKB63	pTS02, *csrA-lacZ*(6)[b], Ap^R	This study
pET28a	T7 overexpression vector, Kn^R	Novagen
pTS02	promoterless *lacZ*, ori pSC101*, Ap^R	[62]
pVP3	pDM4, *phoPQ*::Kan^R	This study
pWH1	pDM4, *phoPQ*$_{YPIII}$	This study

[a] The number indicates the nucleotide of the corresponding gene fused to *lacZ.*

[b] The number indicates the codon of the corresponding gene fused to *lacZ.*

Table 2: Oligonucleotides.

Oligonucleotide	Sequence
555	CGGCGCGGATCCCTCTCACACCAGCTGTG
556	GGGGGCGTCGACGGCAAACTCAATATCCTG
582	GCGGCGGTCGACCCTTCATCCCGTGGTAGG
583	GGGCGCGGATCCGATTGGGCCGGAATCTAGC
774	GCGGCGGAATTCCCTTCATCCCGTGGTAGG
I79	GTCGTCTCCGTTAGAGATTAC
I293	GCTCCGTTTATAGCGTCCTTG
I363	GGGCCGGTCGACCCAATAACAAATTGACTAGC
I617	GGGCGCCTGCAGGCAATGAAGCCGGAACAAATC
II275	GGGGCCCTGCAGCGAGTCAGAATAAGCATTCTTTG
II432	GGCGGCTCGAGCGACATCAATGGCGCTACAC
II433	CGGCGCGTCGACCATTCGCTGTTATCCTCTGTTG
II850	GCGGCGGAGCTCCACTGATGACGAAGTGAGTC
II853	GCGGCGGAGCTCGGTTCTCGCACCTGAGCG
III186	TGTAGTCGGGGACGTTATCG
III187	CCCATCCACCAGCATATAGC
III925	GCGCACTAGTGTCGTGGGTGCCAGCCG
III926	GCGCGAGCTCCCAGCGGCGACGGCCTG
III927	GCGCCTCGAGGTCGTGGGTGCCAGCC
III964	GCCAATGATAACCGTGGTAGTGC
III965	TTTGCACTGTCAGATGGTGACGC
III966	TCTCGACCACTTGGGGCGC
III967	AAAGCCCCTTAGGGGGAGCC
IV703	GCGGGATCCATGCGGGTTCTGGTTGTGG
IV704	GCGAAGCTTTTAGTTGACGTCAAAACGATATCCC
IV937	GATAGTTATAGTTTCTGATGGTC
IV938	GGGCTATTATGCACAGCTCTC
IV939	ATCCATTACGTTCCTTGTATATC
IV940	GAGAGCGTGCATAATAGCCC
V586	GTCGTCTCCGTTAGAGATTAC
V587	GCTCCGTTTATAGCGTCCTTG
V604	GGCTTATGTTTAAGGAACGTAATGGATATACAAGGAACGTAATGGAT ATACAAGGAATGTAATGGATGTACGGGAGCCAAGGA
V605	TCTGACATCCATCCTTGGCTCCTACATTCCTTGTATATCCATTACGTT CCTTGTATATCCATTACGTTCCTTAAACATAAGCC

The corresponding restriction sites are underlined.

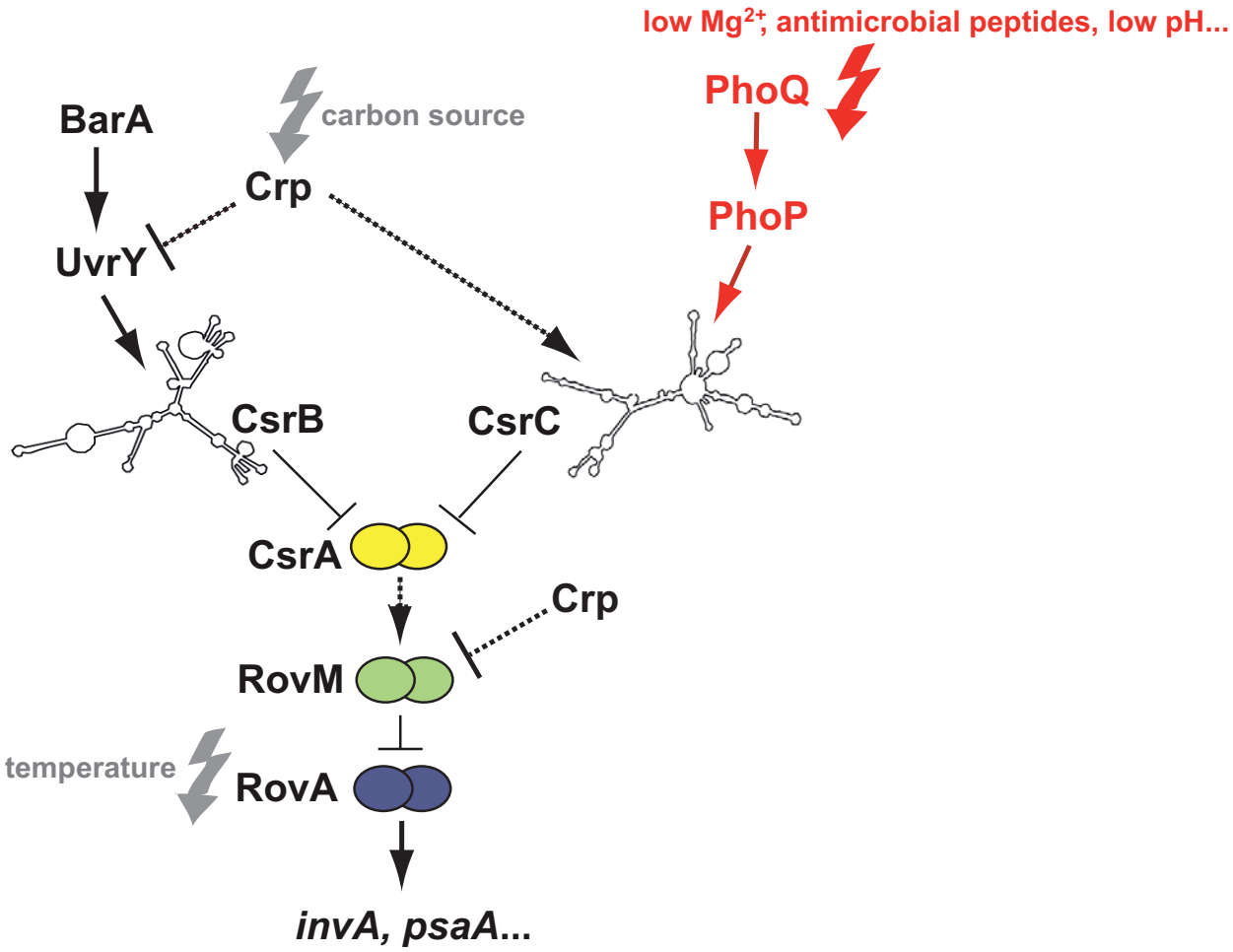

Fig. 1 Nuss *et al*. 2014

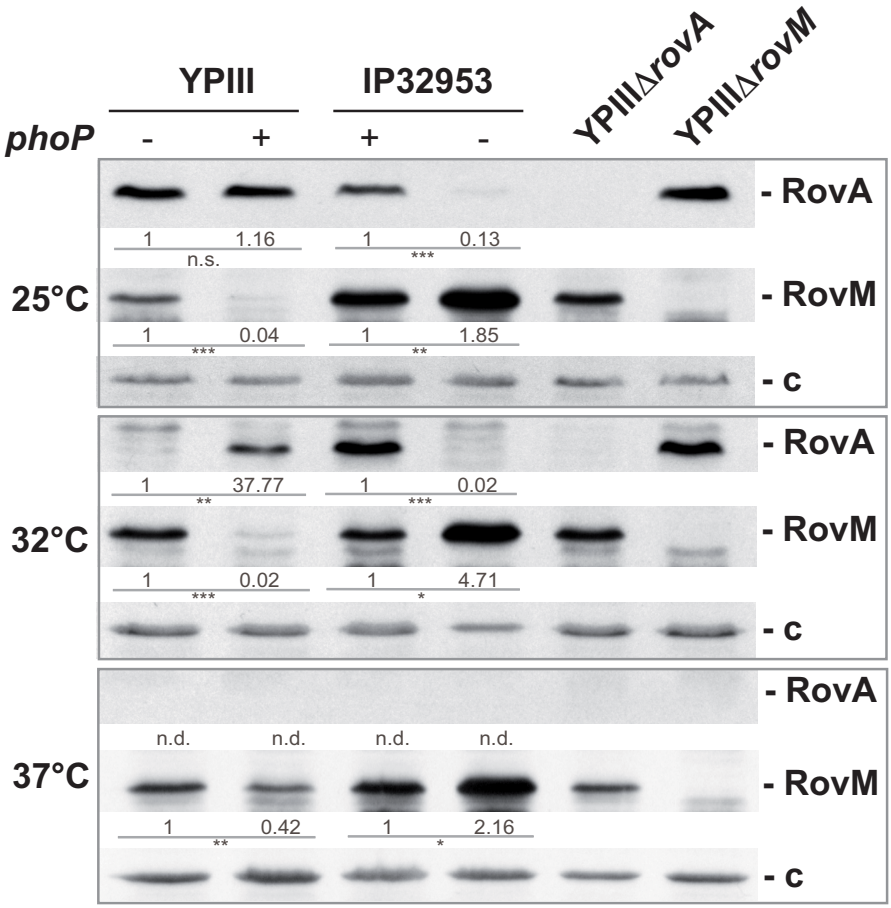

Fig. 2 Nuss *et al*. 2014

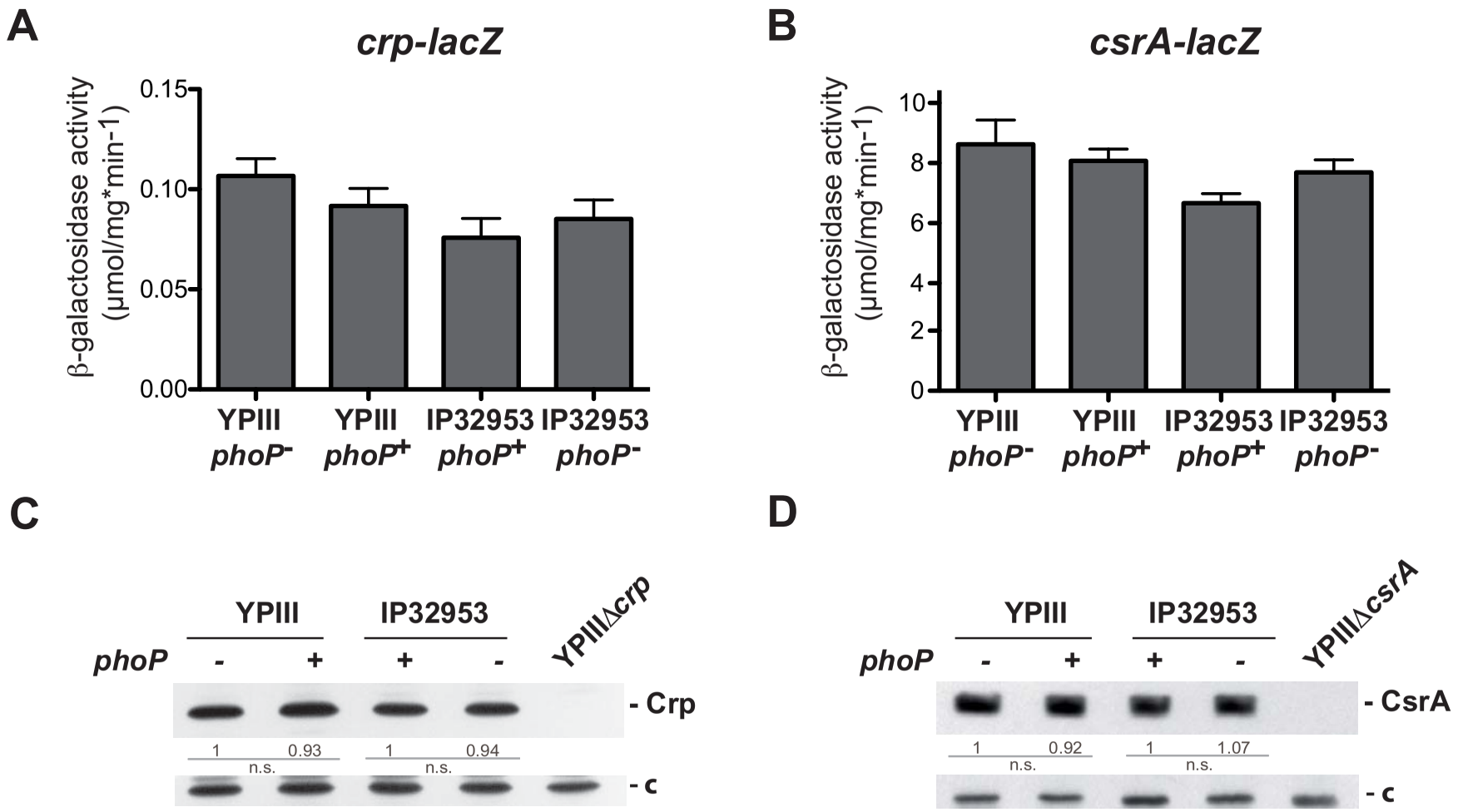

Fig. 3 Nuss *et al.* 2014

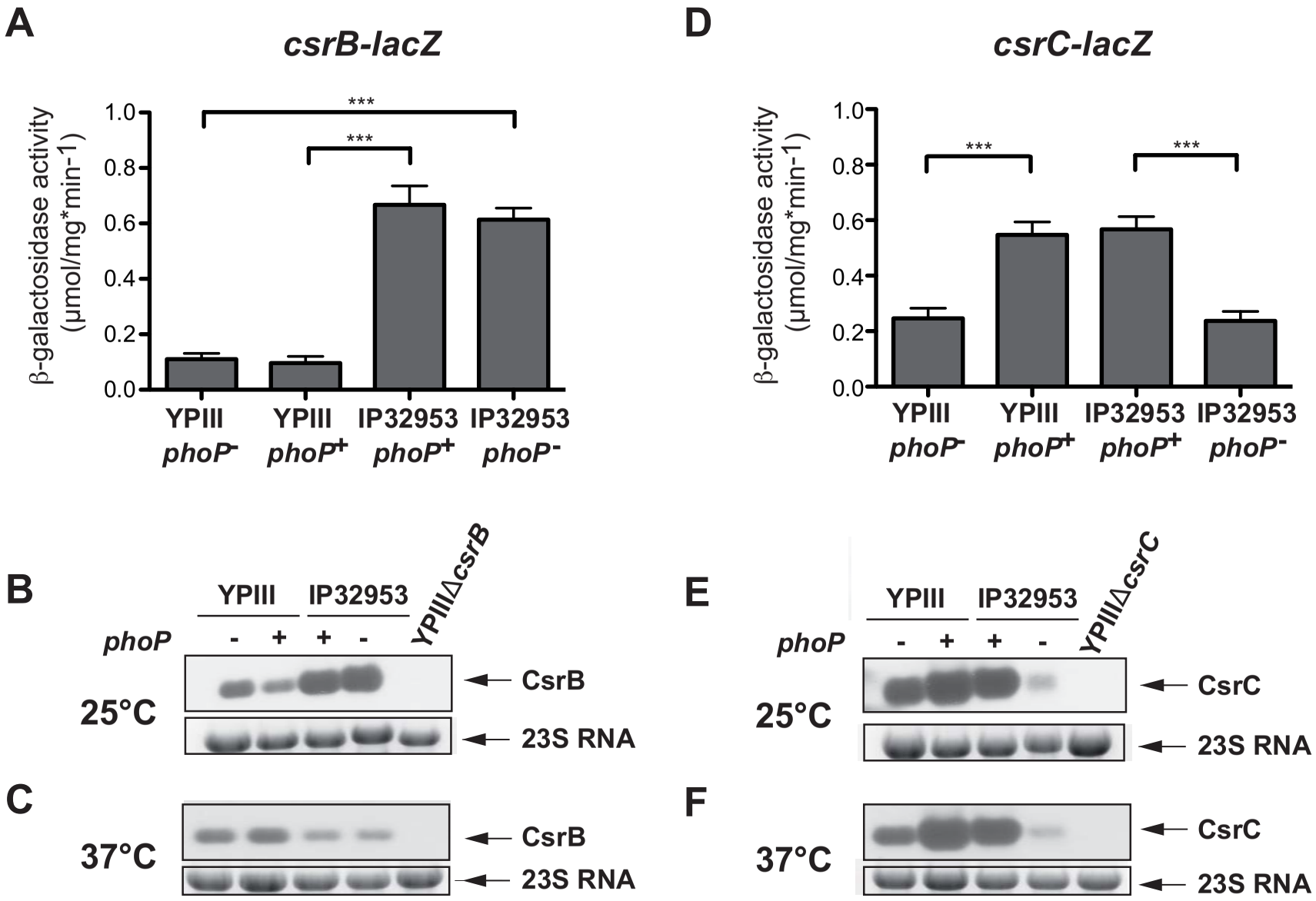

Fig. 4 Nuss *et al.* 2014

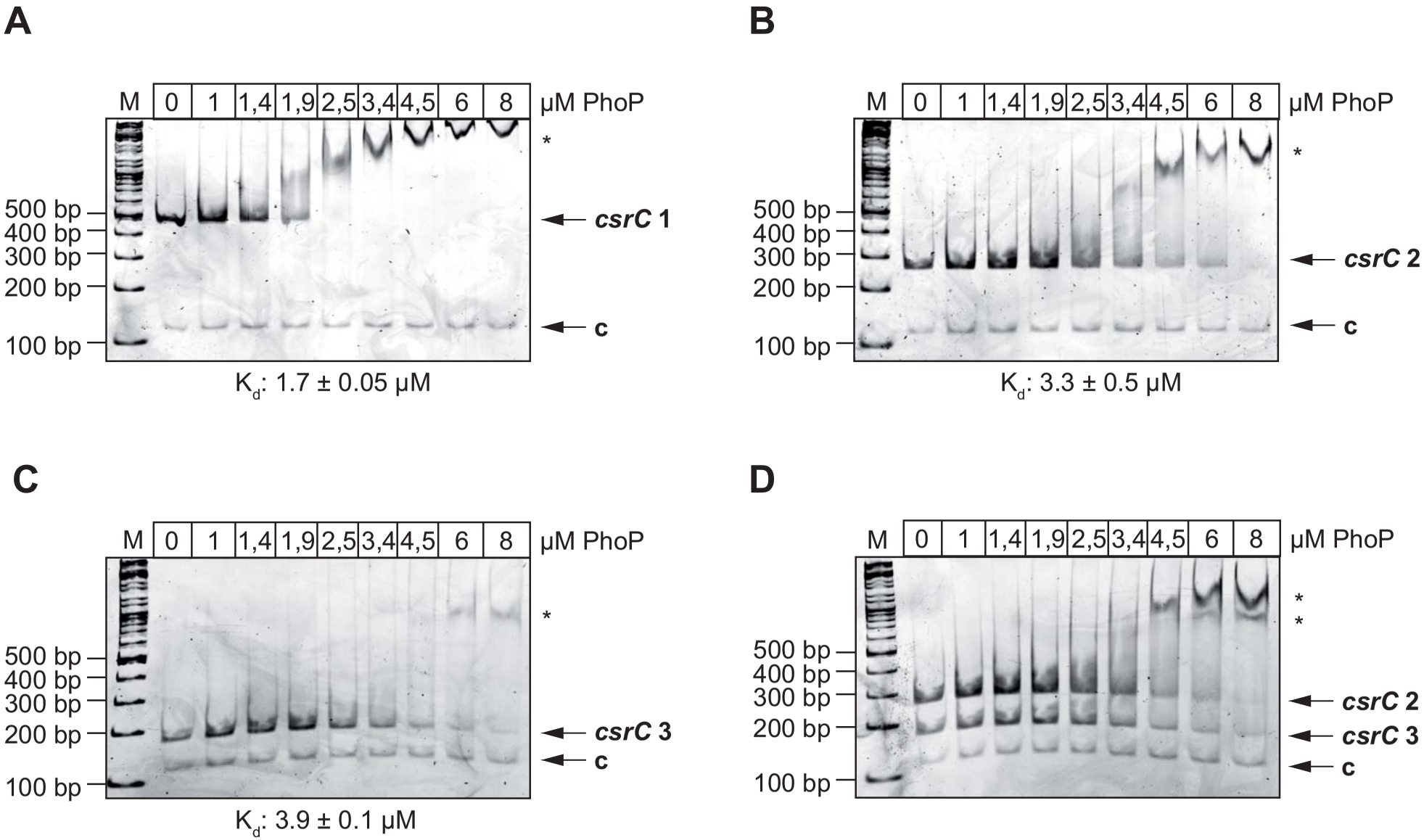

Fig. 5 Nuss *et al*. 2014

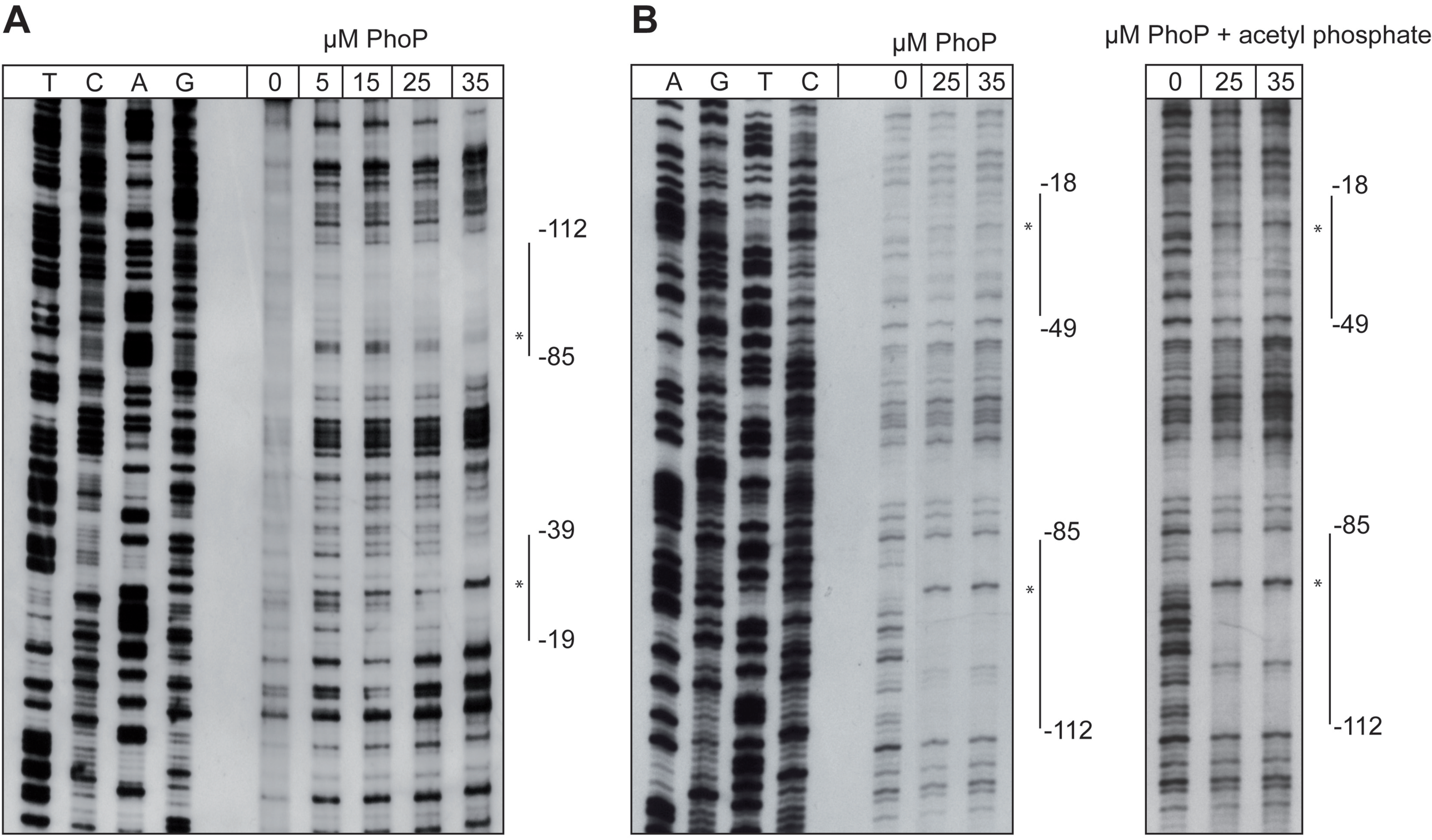

Fig. 6 Nuss *et al*. 2014

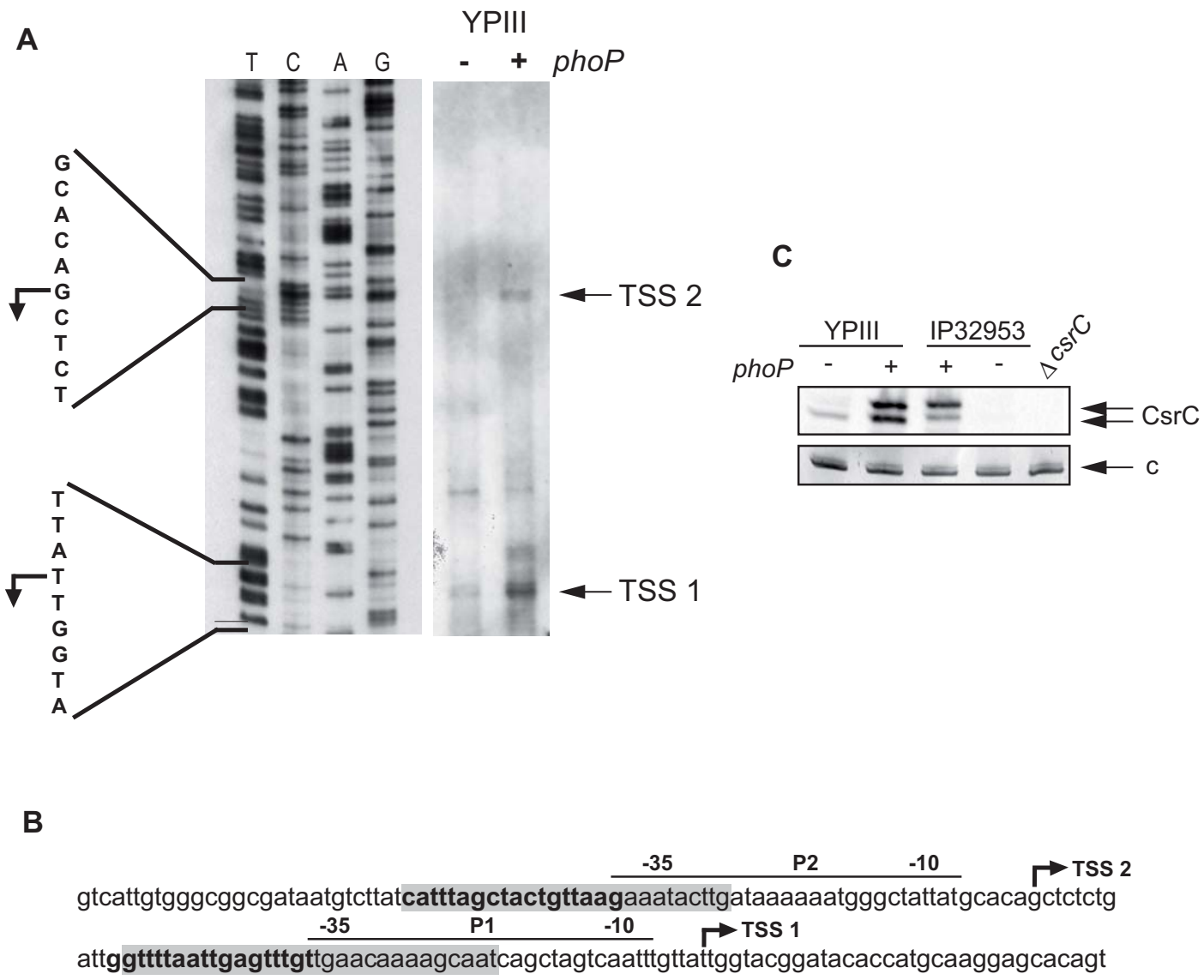

Fig. 7 Nuss *et al*. 2014

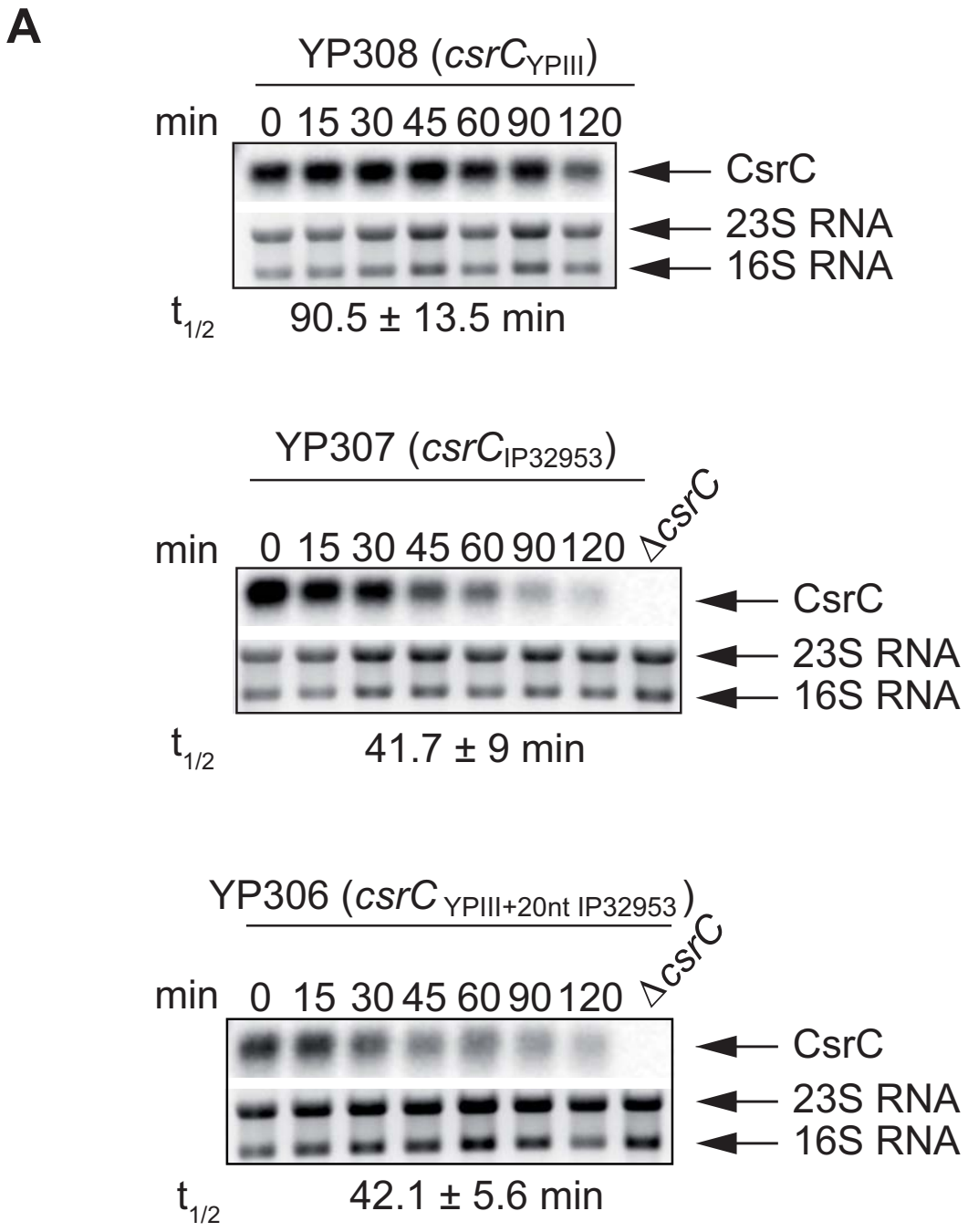

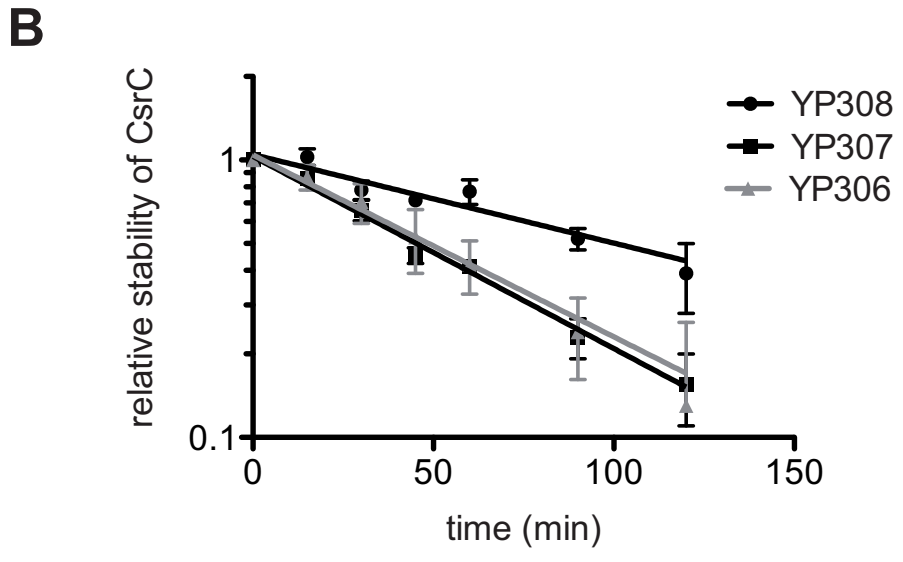

Fig. 8 Nuss *et al*. 2014

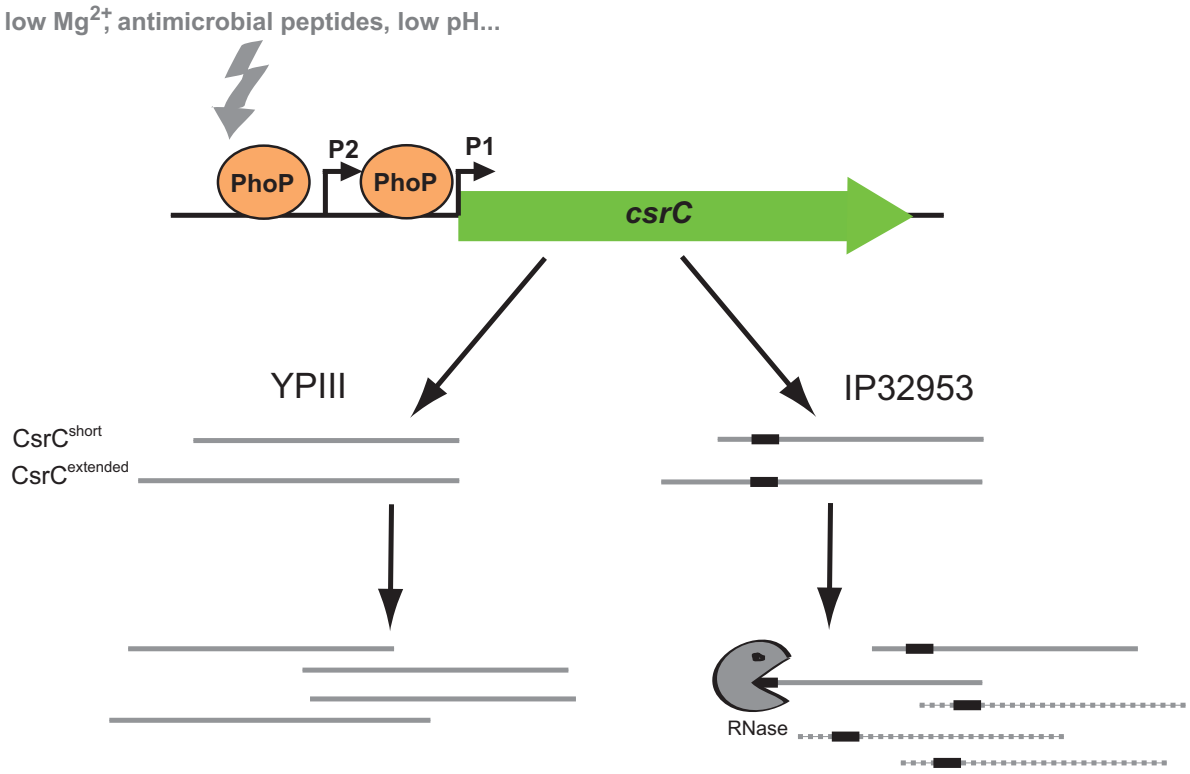

Fig. 9 Nuss *et al.* 2014